

ornl

NUREG/CR-3600
ORNL/TM-9011

**OAK RIDGE
NATIONAL
LABORATORY**

MARTIN MARIETTA

Data Summary Report for Fission Product Release Test HI-4

M. F. Osborne
J. L. Collins
R. A. Lorenz
K. S. Norwood
J. R. Travis
C. S. Webster

Prepared for the
U.S. Nuclear Regulatory Commission
Office of Nuclear Regulatory Research
Under Interagency Agreement DOE 40-551-75

OPERATED BY
MARTIN MARIETTA ENERGY SYSTEMS, INC.
FOR THE UNITED STATES
DEPARTMENT OF ENERGY

Printed in the United States of America. Available from
National Technical Information Service
U.S. Department of Commerce
5285 Port Royal Road, Springfield, Virginia 22161

Available from
GPO Sales Program
Division of Technical Information and Document Control
U.S. Nuclear Regulatory Commission
Washington, D.C. 20555

This report was prepared as an account of work sponsored by an agency of the United States Government. Neither the United States Government nor any agency thereof, nor any of their employees, makes any warranty, express or implied, or assumes any legal liability or responsibility for the accuracy, completeness, or usefulness of any information, apparatus, product, or process disclosed, or represents that its use would not infringe privately owned rights. Reference herein to any specific commercial product, process, or service by trade name, trademark, manufacturer, or otherwise, does not necessarily constitute or imply its endorsement, recommendation, or favoring by the United States Government or any agency thereof. The views and opinions of authors expressed herein do not necessarily state or reflect those of the United States Government or any agency thereof.

NUREG/CR-3600
ORNL/TM-9011
Dist. Category R3

Chemical Technology Division

DATA SUMMARY REPORT FOR FISSION PRODUCT RELEASE TEST HI-4

M. F. Osborne
J. L. Collins
R. A. Lorenz
K. S. Norwood
J. R. Travis
C. S. Webster

Manuscript Completed — November 1983
Date of Issue — June 1984

NOTICE This document contains information of a preliminary nature.
It is subject to revision or correction and therefore does not represent a
final report.

Prepared for the
U.S. Nuclear Regulatory Commission
Office of Nuclear Regulatory Research
Washington, DC 20555
under Interagency Agreement DOE 40-551-75

NRC FIN No. B0127

Prepared by the
OAK RIDGE NATIONAL LABORATORY
Oak Ridge, Tennessee 37831
operated by
MARTIN MARIETTA ENERGY SYSTEMS, INC.
for the
U.S. DEPARTMENT OF ENERGY
under Contract No. DC-AC05-84OR21400

•

•

•

•

•

•

ABSTRACT

The fourth in a series of high-temperature fission product release tests was conducted in which a 20.3-cm-long fuel specimen from the Peach Bottom-2 reactor was heated for 20 min at a maximum temperature of $\sim 1850^{\circ}\text{C}$ in a flowing steam-helium atmosphere. The test specimen was part of a fuel rod which was irradiated to ~ 10.10 MWd/kg.

Posttest metallographic examination of the fuel specimen revealed evidence of cladding melting at each of the transverse cuts that were made. Gas analysis during the test indicated that $\sim 54\%$ of the cladding was oxidized. Total oxidation did not occur because of the low steam flow which was used.

Gamma spectrometry (GS) and neutron activation (NA) analyses of test components revealed the following releases: (1) GS — 21.1% ^{85}Kr , 31.7% ^{137}Cs ; and (2) NA — 24.7% ^{129}I (percentages of the total calculated segment inventories). A value of 35.8% cesium release was determined by counting the fuel rod segment before and after the test. If the pellet-clad gap fission gas inventory had also been available for release in the test, the ^{85}Kr release would have been 31.3% .

Significant releases of radiogenic Rb, Cd, Ag, and Br, as well as trace amounts of Te, La, Ba, Sr, and Eu, were detected by spark-source mass spectrometric analysis.

The masses of materials which were transported by carrier gas to the thermal gradient tube (TGT) and filters from the furnace and test specimen were measured by weighing. The concentrations of vapor and aerosol particulates in the gas stream were calculated from these weights.

•

•

•

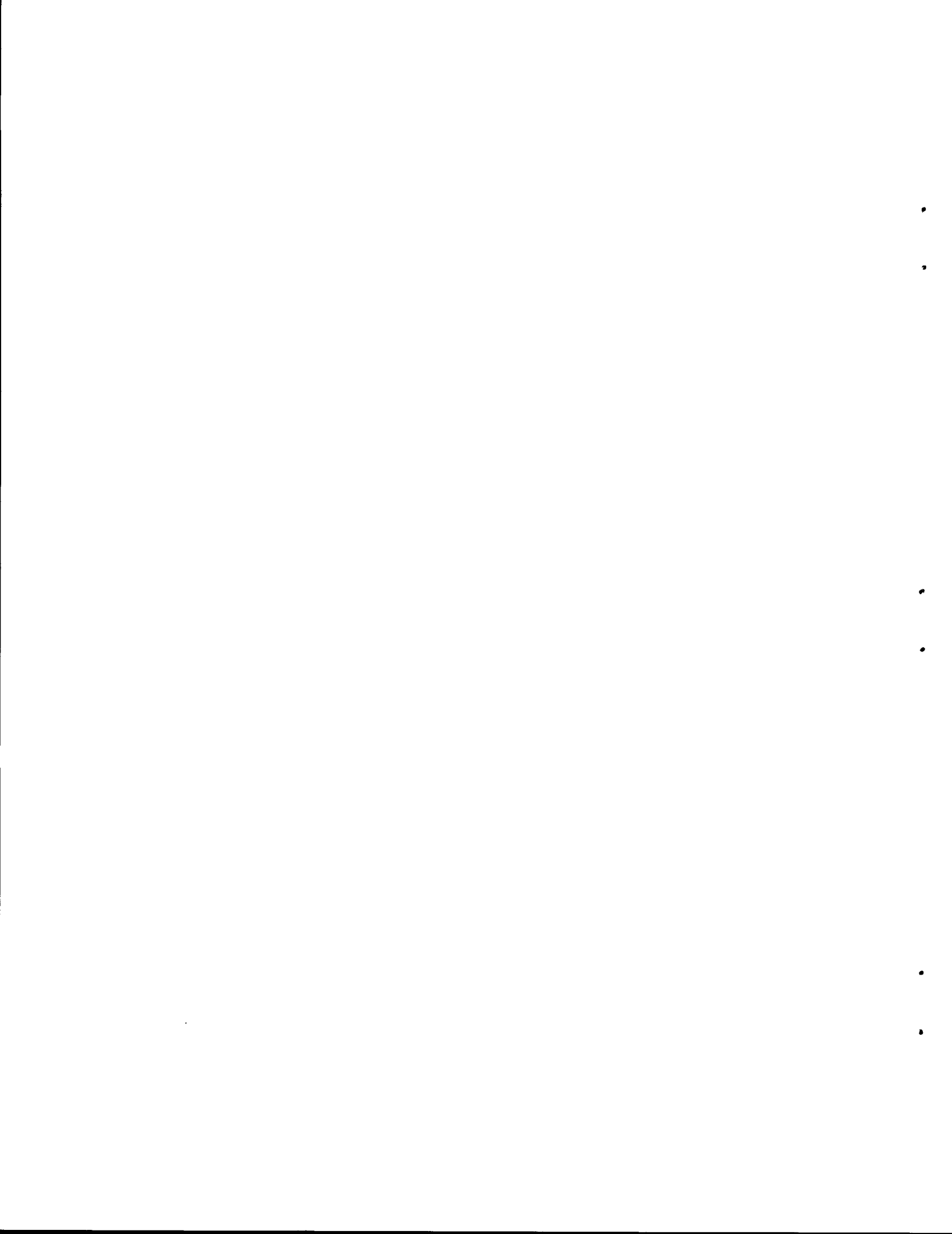
•

•

•

CONTENTS

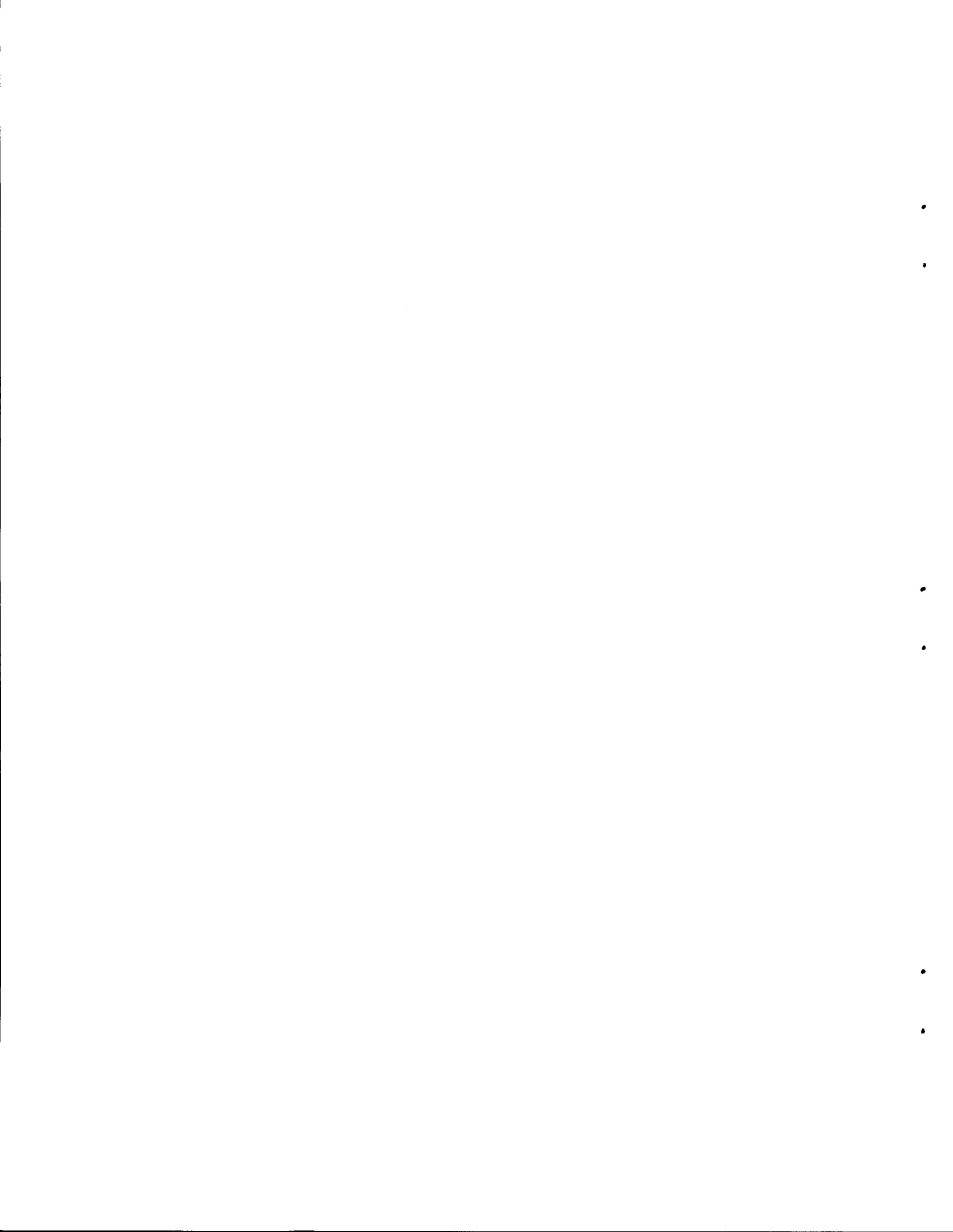
	<u>Page</u>
ABSTRACT	iii
FOREWORD	vii
ACKNOWLEDGMENTS	ix
LIST OF FIGURES	xi
LIST OF TABLES	xiii
1. INTRODUCTION	1
2. TEST DESCRIPTION	2
2.1 CHARACTERISTICS OF THE PEACH BOTTOM-2 REACTOR FUEL AND TEST SPECIMEN	2
2.2 FISSION GAS RELEASE DURING IRRADIATION	2
2.3 EXPERIMENTAL APPARATUS	12
2.4 TEST CONDITIONS AND OPERATION	12
2.5 POSTTEST DISASSEMBLY AND SAMPLE COLLECTION	20
3. TEST RESULTS	21
3.1 TEST DATA	21
3.2 POSTTEST DATA	21
3.2.1 Results from Gamma Spectrometry	25
3.2.2 Results of Activation Analysis for Iodine	27
3.2.3 Results of SSMS Analysis	27
3.2.4 Thermal Gradient Tube Results	35
3.2.4.1 Interpretation: cesium and iodine on the thermal gradient tube	44
3.2.5 Aerosol Characteristics	45
3.2.6 Metallographic Examination of Fuel Specimen	46
3.2.7 Determination of Cesium Release by Gamma-ray Spectrometric Counting of the Fuel Rod Segment Before and After Test HI-4	51
4. CONCLUSIONS	57
5. REFERENCES	58



FOREWORD

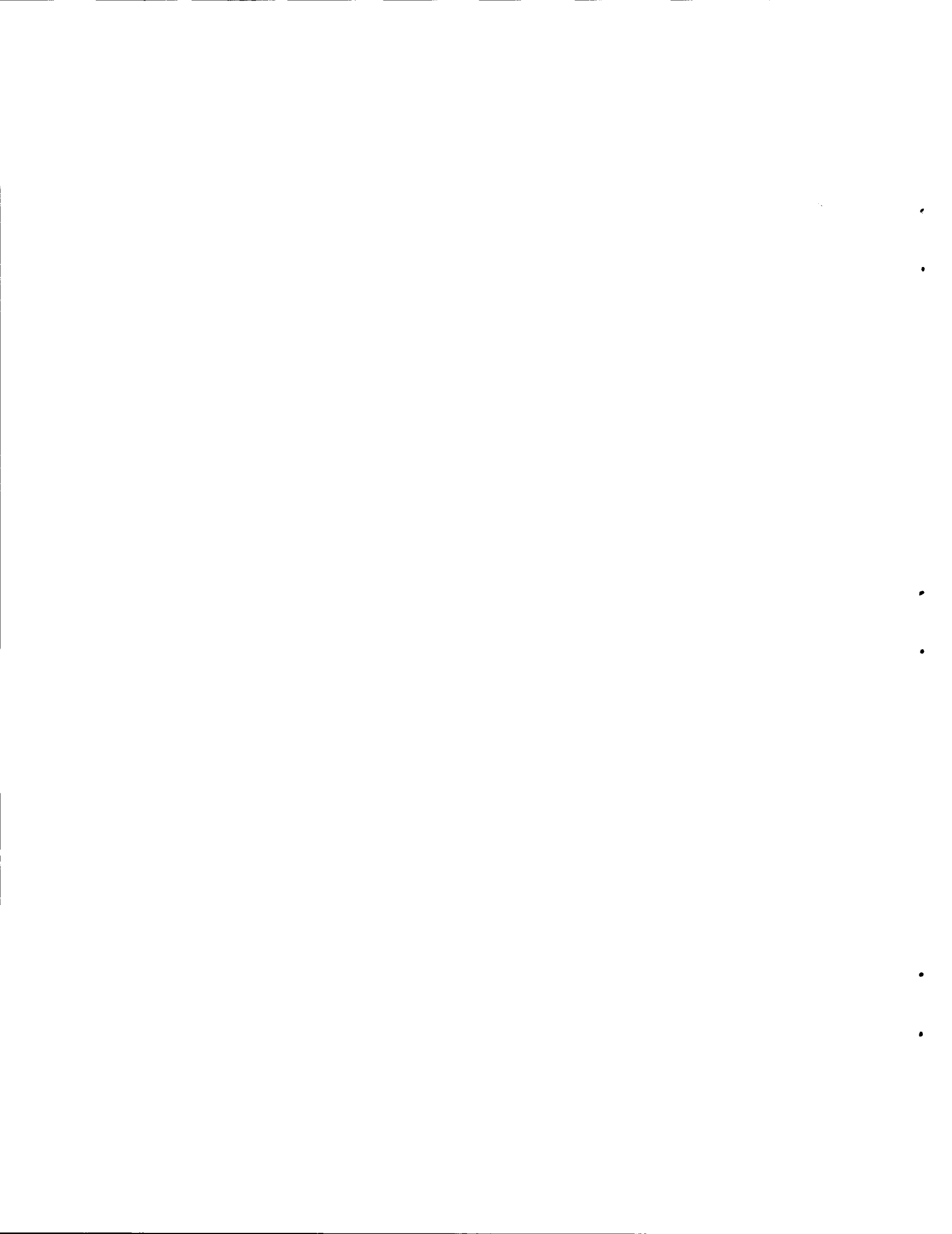
This document is the fourth in a series of reports describing the conduct and results of fission product release testing of commercial LWR fuel. The other reports are:

1. M. F. Osborne, R. A. Lorenz, J. R. Travis, and C. S. Webster, Data Summary Report for Fission Product Release Test HI-1, NUREG/CR-2928 (ORNL/TM-8500), December 1982.
2. M. F. Osborne, R. A. Lorenz, J. R. Travis, C. S. Webster, and K. S. Norwood, Data Summary Report for Fission Product Release Test HI-2, NUREG/CR-3171 (ORNL/TM-8667), February 1984.
3. M. F. Osborne, R. A. Lorenz, K. S. Norwood, J. R. Travis, and C. S. Webster, Data Summary Report for Fission Product Release Test HI-3, NUREG/CR-3335 (ORNL/TM-8793), April 1984.



ACKNOWLEDGMENTS

The authors gratefully acknowledge the significant contributions of several colleagues in conducting this work: D. A. Costanzo, J. Northcutt, L. Hall, and L. Landau of the Analytical Chemistry Division for the ^{129}I determinations and spark-source mass spectrometry; L. Shrader of the Metals and Ceramics Division for metallographic examination; R. P. Wichner and T. B. Lindemer for technical consultation; B. C. Drake for preparation of the manuscript; and D. R. Reichle for editing.



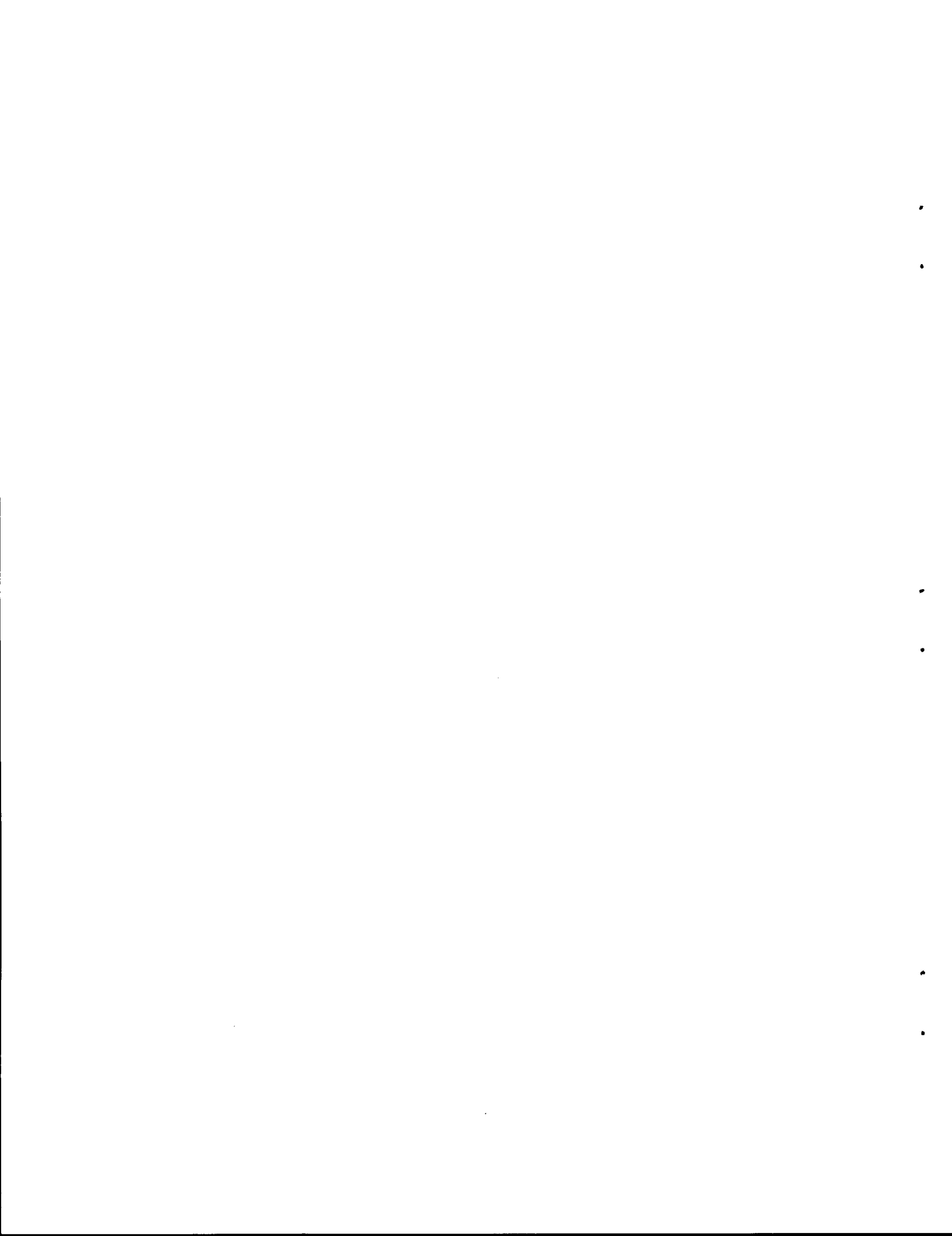
LIST OF FIGURES

<u>Number</u>		<u>Page</u>
1.	Gamma scan of rod F-6 from bundle PH-006, Peach Bottom-2 reactor. The test HI-4 specimen was cut from segment 7	6
2.	Fuel specimen for fission product release studies	7
3.	Stable fission gas release estimated as a function of linear heat rating. (<u>Source</u> : ref. 13)	10
4.	Fission product release furnace	13
5.	Fission product release and collection system	14
6.	Photograph of (a) fission product release furnace, (b) thermal gradient tube, and (c) filter package in steel containment box before test HI-2	15
7.	Fission product collection system	16
8.	Data acquisition and processing system for fission product release test	17
9.	Temperature and flow history of test HI-4	22
10.	Estimated temperature profile of fuel rod segment during test HI-4	23
11.	Collections of ^{85}Kr and ^{137}Cs as functions of temperature and time in test HI-4	24
12.	Distribution of cesium and iodine in test HI-4	28
13.	Distribution of fission products cesium and iodine and total deposited material in the thermal gradient tube in test HI-4. (The temperature profile is given in Fig. 16.)	32
14.	Distribution of fission products cesium, iodine, and cadmium in the thermal gradient tube in test HI-4, as determined by SSMS analysis. (The temperature profile is given in Fig. 16.)	33
15.	Distribution of major contaminants along the thermal gradient tube after test HI-4, as determined by SSMS analysis. (The temperature profile is given in Fig. 16.)	34
16.	Temperature distribution along thermal gradient tube in test HI-4	36
17.	Cesium profile along thermal gradient tube in test HI-4	39

<u>Number</u>		<u>Page</u>
18.	Cesium profile along thermal gradient tube in test HI-4 as a function of the temperature of the deposition surface	40
19.	Iodine profile along thermal gradient tube in test HI-4	41
20.	Iodine profile along thermal gradient tube in test HI-4 as a function of the temperature of the deposition surface	42
21.	Solubility of cesium deposited in the thermal gradient tube of test HI-4: comparison of basic and acidic leaches	43
22.	Appearance of filters from test HI-4; from the left, screen covering glass wool prefilter, first HEPA, and second HEPA ..	47
23.	Sections of fuel specimen and ZrO ₂ ceramics from test HI-4; sections were cut at 1-in. intervals, with cut 1 at the inlet end	49
24.	Transverse sections from test HI-4 that were examined metallographically. The numbers 1, 2, and 3 identify areas photographed, some of which are shown in Fig. 25	50
25.	View of area 2, section 0 in Fig. 24, showing interaction zones at molten cladding/UO ₂ interface (above) and molten cladding ZrO ₂ boat interface (below)	52
26.	Higher-magnification view of area from upper region in Fig. 24, showing two metallic phases	53
27.	View of a small region from area 3 of section 3 (see Fig. 24) showing large voids in the previously molten cladding and penetration of the melt into a crack in the UO ₂ . The cladding contains ZrO ₂ plus other unidentified phases	54
28.	Higher-magnification view of melted cladding region above the large void on the left in Fig. 27. Gray phase is ZrO ₂ ; metallic phases probably are (U,Zr) alloy and α-U,Zr(O)	55
29.	View of area 2, section 7 (see Fig. 24), showing projections from cladding which were observed in several regions of this section. These projections contain a small fraction of ZrO ₂ plus two other unidentified phases	56

LIST OF TABLES

<u>Number</u>		<u>Page</u>
1.	Data for fuel specimen used in test HI-4	3
2.	Amounts of principal fission and activation product elements in Peach Bottom-2 reactor fuel and cladding after 1937 d of decay	4
3.	Principal radionuclides and selected stable nuclides in Peach Bottom-2 reactor fuel and cladding after 1937 d of decay	5
4.	Analysis of gas removed from plenum and void spaces of Peach Bottom-2 fuel rod DG-2986	8
5.	Fission gas found in the plenum of Peach Bottom-2 rod DG-2986	9
6.	Axial distribution of burnup and fission gas release for Peach Bottom-2 reactor fuel	11
7.	Comparison of apparatus and test conditions for the four HI tests	18
8.	Operating conditions for test HI-4	19
9.	Distribution and fractional release of fission products in test HI-3	25
10.	Distribution of cesium in test HI-4	26
11.	Fractional release and distribution of iodine in test HI-4 (Results of activation analysis for ¹²⁷ I)	29
12.	Results of SSMS analysis of samples from test HI-4	31
13.	Fission product release as determined by SSMS	35
14.	Fission products on thermal gradient tube in test HI-4	38
15.	Aerosol particles and vapor produced in fission product release tests	48



DATA SUMMARY REPORT FOR FISSION PRODUCT RELEASE TEST HI-4

M. F. Osborne
J. L. Collins
R. A. Lorenz
K. S. Norwood
J. R. Travis
C. S. Webster

1. INTRODUCTION

This report summarizes data from the fourth test in a series designed to investigate fission product release from LWR fuel in steam throughout the temperature range 1400 to ~2400°C.¹ Earlier tests, conducted under similar conditions at temperatures of 500 to 1600°C, have been reported by Lorenz et al.²⁻⁵ The purpose of this work, which is sponsored by the U.S. Nuclear Regulatory Commission (NRC), is to obtain the experimental data needed to reliably assess the consequences of heatup accidents in light water reactors. The primary objectives of this program are:

1. to determine fission product release from discharged LWR fuel at temperatures up to and including fuel melting (~2400°C);
2. to identify, to the extent possible, the chemical species of the released fission products;
3. to compare the observed fission product behavior with the physical and chemical changes in the fuel specimens;
4. to correlate the results with data from related programs and develop a consistent source term model applicable to any LWR fuel subjected to a spectrum of accident conditions.

Tests of high-burnup LWR fuel are emphasized in this program; however, the applicability of simulated fuel (unirradiated UO₂ containing a range of fission product elements) will also be investigated, but only at test temperatures >2000°C. As in the first four tests, all remaining tests will be conducted in a flowing mixture of steam and helium (or argon) at atmospheric pressure; steam concentrations will be varied to simulate different accident sequences or core locations.

Test temperatures in the existing induction furnace are limited by material properties to a maximum of ~2000°C. Higher-temperature tests are planned but will require the replacement of the currently used ZrO₂ ceramics with ThO₂. In addition, the existing fission product collection and analysis system will be expanded to provide broader sampling capability with the higher-temperature furnace.

This report provides a brief description of test HI-4 and a summary of the results obtained. As noted in the previous data summary reports,⁶⁻⁸ thorough data evaluation and correlation will be included in a subsequent topical report covering the first series of fission product release tests at temperatures up to 2000°C.

2. TEST DESCRIPTION

The objective of test HI-4 was to obtain release data at $\sim 1800^{\circ}\text{C}$ for a period of 20 min in a steam atmosphere.

2.1 CHARACTERISTICS OF THE PEACH BOTTOM-2 REACTOR FUEL AND TEST SPECIMEN

The test specimen was a 20.3-cm-long section from rod F-6 from assembly PH-006, which operated in the Peach Bottom-2 reactor from January 12, 1974, to March 26, 1976.^{9,10} Details of the irradiation and of the characteristics of this particular specimen are listed in Table 1; calculated fission product inventories for the specimen are shown in Tables 2 and 3.

An axial scan of the total gamma radioactivity in the energy range 0.55 to 0.75 MeV is shown in Fig. 1. These scan measurements were made 2.25 years after shutdown. The scan primarily shows the distribution of radioactive cesium.¹¹ Segment numbers correspond to 30.5-cm (12-in.) lengths that were cut for each test specimen used in a prior study.⁴ Segment 11 was dissolved, and the burnup was estimated to be 7.730 MWd/kg.¹² For this test (HI-4), a 20.3-cm (8-in.)-long section (coded-P-7) was used which was cut from segment 7 (Fig. 2). The estimated burnup for the specimen was 10.10 MWd/kg. Burnups calculated from the analysis of segment 11 and used in ref. 12 are not considered to be as accurate as those given in this report. Tapered end caps of Zircaloy-2 were pressed onto the ends of the specimen, not as gas seals, but to prevent loss of the fractured UO_2 fuel during subsequent handling. A small hole, 1.6 mm in diameter, was drilled through the cladding at mid-length to serve as a standard outlet for fission product release during the test.

2.2 FISSION GAS RELEASE DURING IRRADIATION

Fuel rod DG-2986 was punctured, and the contents of the plenum and void spaces were analyzed by EG&G Idaho.¹³ The results of the analysis are presented in Table 4. By using an evacuation and gas backfill technique, the total void volume was measured as 74.0 cm^3 ; this compares well with the volume calculated from the data in Table 1: plenum volume = 51.2 cm^3 , gap volume = 21.6 cm^3 , and pellet-end void volume = 3.3 cm^3 , for a total of 76.1 cm^3 .

Using the ORIGEN-calculated inventory and assuming an average rod burnup of 8.388 MWd/kg, the 99.9 cm^3 of krypton and xenon gas is equivalent to 9.12% release of the total inventory to the plenum and void spaces during irradiation. The isotopic releases are given in Table 5.

To estimate gap inventories of cesium and iodine, it was necessary to calculate the fission gas released from the individual test segments of the fuel rod. A previously determined correlation that showed gas release as a function of irradiation time and linear heat rating¹⁴ was used to predict the inventory fraction release (see Fig. 3). The axial linear power distribution was assumed to be the same as the burnup distribution given in Table 6. In order to obtain the total fission gas release of 9.12%, it was necessary to assume that segment 5 (section with peak burnup) operated

Table 1. Data for fuel specimen used in test HI-4

Fuel rod identification	Serial number — DG-2986 Assembly type 1, rod type 1, location F-6 in assembly PH-006
Irradiation data:	
Period	Jan. 12, 1974, to May 26, 1976 (cycle 1)
Average burnup of rods in core	~10.00 MWd/kg
Average burnup of rod DG-2986	~8.388 MWd/kg
Burnup of 20.3-cm-long test specimen	10.10 MWd/kg
Fuel rod characteristics (unirradiated):	
Zircaloy-2 cladding	1.430 cm (0.563 in.) OD 1.267 cm (0.499 in.) ID
Pellet	1.237 cm (0.487 in.) diam
Initial radial gap	0.015 cm (0.0059 in.)
Plenum length	40.64 cm (16.0 in.)
UO ₂ density	10.42 g/cm ³
Initial enrichment	1.33% ²³⁵ U ^a
UO ₂ stack density	10.34 g/cm ³
UO ₂ stack length	365.8 cm (144.0 in.)
UO ₂ stack mass	4548 g
U stack mass	4009 g
Test specimen characteristics:	
Length	20.3 cm (8.0 in.)
Location	~180.5 to 200.8 cm from bottom end of rod
Specimen fuel loading	254.6 g UO ₂ (224.4 g U)
Total weight of specimen	306 g
Weight of Zircaloy cladding and end caps	51.4 g

^aMost fuel rods in the core were of higher enrichment.

Table 2. Amounts of principal fission and activation product elements in Peach Bottom-2 reactor fuel and cladding after 1937 d of decay^a

Element	Mass		Element	Mass	
	g/MT	HI-4 specimen ^b (mg)		g/MT	HI-4 specimen (mg)
Mn	7.74	1.74	In	2.296	0.515
Co	3.91	0.878	Sn ^c	4915	1103
Se	18.87	4.23	Sb ^d	10.31	2.315
Br	7.464	1.67	Te ^e	173.9	39.02
Kr	117.1	26.28	I	89.12	20.00
Rb	111.6	25.04	Xe	1786	400.8
Sr	263.3	59.09	Cs	917.2	205.8
Y	145.8	32.72	Ba	514.8	115.5
Zr	299,700	67,240	La	411.8	92.41
Mo	1195	268.1	Ce	791.9	177.7
Tc	279.7	62.76	Pr	391.5	87.85
Ru	753.0	168.97	Nd	1347	302.3
Rh	206.2	46.27	Pm	19.17	4.30
Pd	482.4	108.3	Sm	287.7	64.56
Ag	33.60	7.54	Eu	40.84	9.16
Cd	60.48	13.57	Gd	25.46	5.17
Total of all fission products	11,620	2606			
Total of all activation products	304,900	68,420			
U	9.891+15	2.203+5			
²³⁵ U	6.254+3	1.403+3			
Pu	6.242+3	1.401+3			

^a Calculated by C. W. Alexander using the ORIGEN computer program, with a burnup of 10.1 MWd/kg and a 1937-d decay to July 15, 1981.

^b Original uranium content of 20.3-cm fuel specimen was 224.4 g; initial enrichment was 1.33% ²³⁵U. Thus, the fuel specimen was 0.02244% of a metric ton.

^c For 1 metric ton of initial uranium, there are: 298.5 kg cladding Zr and 1.173 kg fission product Zr, 4875 g cladding Sn and 33.80 g fission product Sn.

^d Cladding activation provides 15% of the total antimony mass.

^e The tellurium is 73.0 wt % ¹³⁰Te and 23.4 wt % ¹²⁸Te. Tellurium-125 makes up most of the remainder.

Table 3. Principal radionuclides and selected stable nuclides in Peach Bottom-2 reactor fuel and cladding after 1937 d of decay^a

Nuclide	Amount 'per 1000 kg of initial uranium		Amount in HI-4 specimen ^b	
	(Ci)	(g)	(mCi)	(mg)
⁵⁴ Mn	0.358	4.6×10^{-5}	0.0	1.4×10^{-5}
⁶⁰ Co	119.9	0.1060	26.90	2.4×10^{-2}
⁸³ Kr	0.0	15.59	0.0	3.498
⁸⁴ Kr	0.0	34.85	0.0	7.820
⁸⁵ Kr	2190	5.580	491.4	1.252
⁸⁶ Kr	0.0	60.84	0.0	13.65
⁹⁰ Sr	20,650	151.3	4634	33.95
⁹³ Zr ^c	0.6949	276.4	0.156	62.02
⁹⁹ Tc	4.744	279.7	1.065	62.77
¹⁰⁶ Ru	5929	1.77	1331	0.397
¹¹⁰ mAg	4.494	9.5×10^{-4}	1.008	2.1×10^{-4}
¹¹³ mCd	15.0	0.069	3.366	0.016
¹²⁵ Sb ^c	1876	1.815	421.0	0.4074
¹²⁹ I	1.2×10^{-2}	67.56	2.7×10^{-3}	15.16
¹²⁵ Xe	0.0	0.552	0.0	0.124
¹³⁰ Xe	0.0	2.25	0.0	0.505
¹³¹ Xe	0.0	180.0	0.0	40.39
¹³² Xe	0.0	343.9	0.0	77.171
¹³⁴ Xe	0.0	496.9	0.0	111.5
¹³⁶ Xe ^d	0.0	762.3	0.0	171.16
¹³⁴ Cs ^d	4864	3.758	1092	0.843
¹³⁷ Cs ^d	31,590	363.0	7089	81.46
¹⁴⁴ Ce	4034	1.264	905.2	0.284
¹⁴⁷ Pm	17,770	19.17	3988	
¹⁵¹ Sm	193.1	7.337	43.3	1.646
¹⁵⁴ Eu	1420	5.257	318.7	1.180
¹⁵⁵ Eu	855.2	1.838	191.9	0.412
Total	152,500	11,660	34,220	2,617

^aCalculated by C. W. Alexander using the ORIGEN computer program, with a burnup of 10.1 MWd/kg and a 1937-d decay to July 15, 1981.

^bOriginal uranium content of 20.3-cm fuel specimen was 224.4 g; initial enrichment was 1.33% ²³⁵U.

^cCladding activation contributes 13.9% of ⁹³Zr and 16.1% of ¹²⁵Sb.

^dActivity ratio for cesium (Ci ¹³⁷Cs per Ci ¹³⁴Cs) = 6.495. Isotopic composition is 45.3 wt % ¹³³Cs, 0.4 wt % ¹³⁴Cs, 14.7 wt % ¹³⁵Cs, and 39.6 wt % of ¹³⁷Cs.

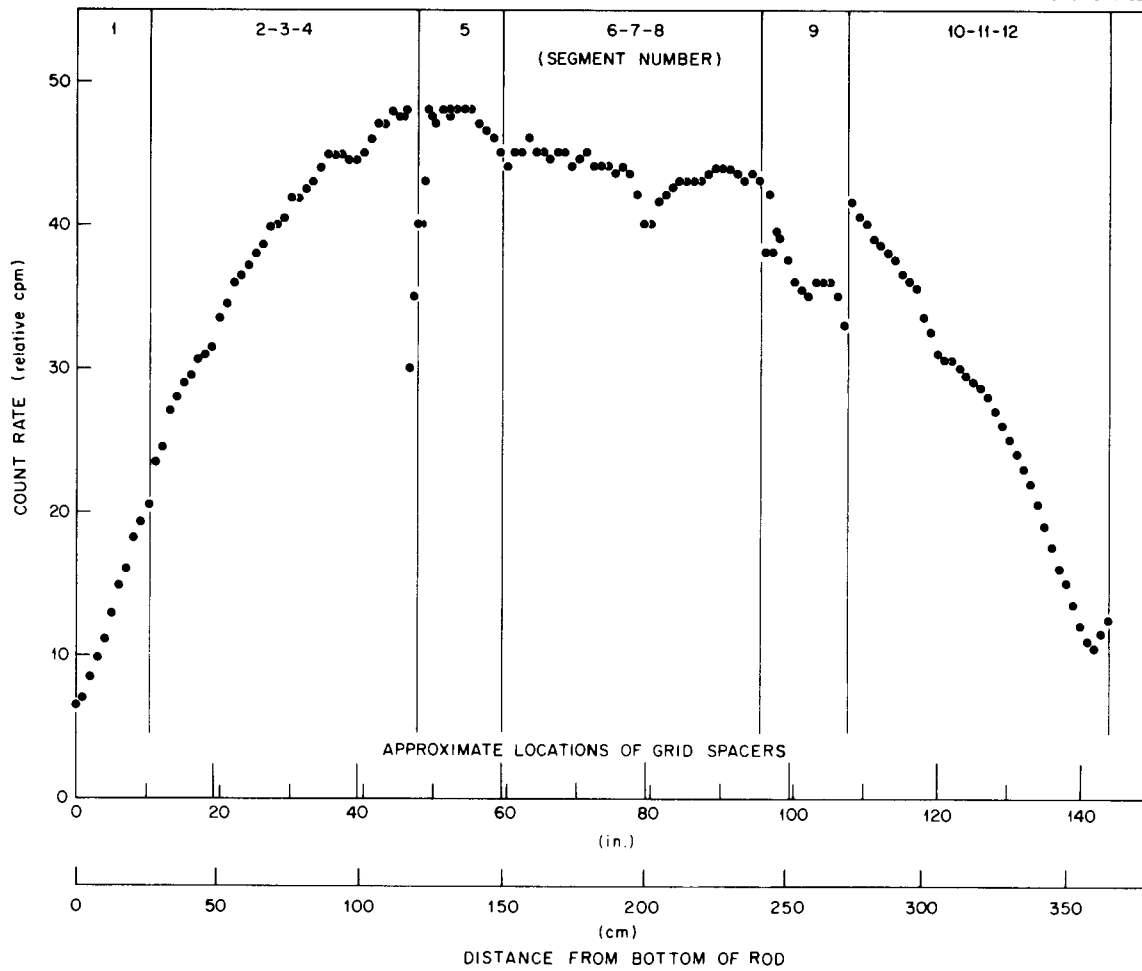


Fig. 1. Gamma scan of rod F-6 from bundle PH-006, Peach Bottom-2 reactor. The test HI-4 specimen was cut from segment 7.

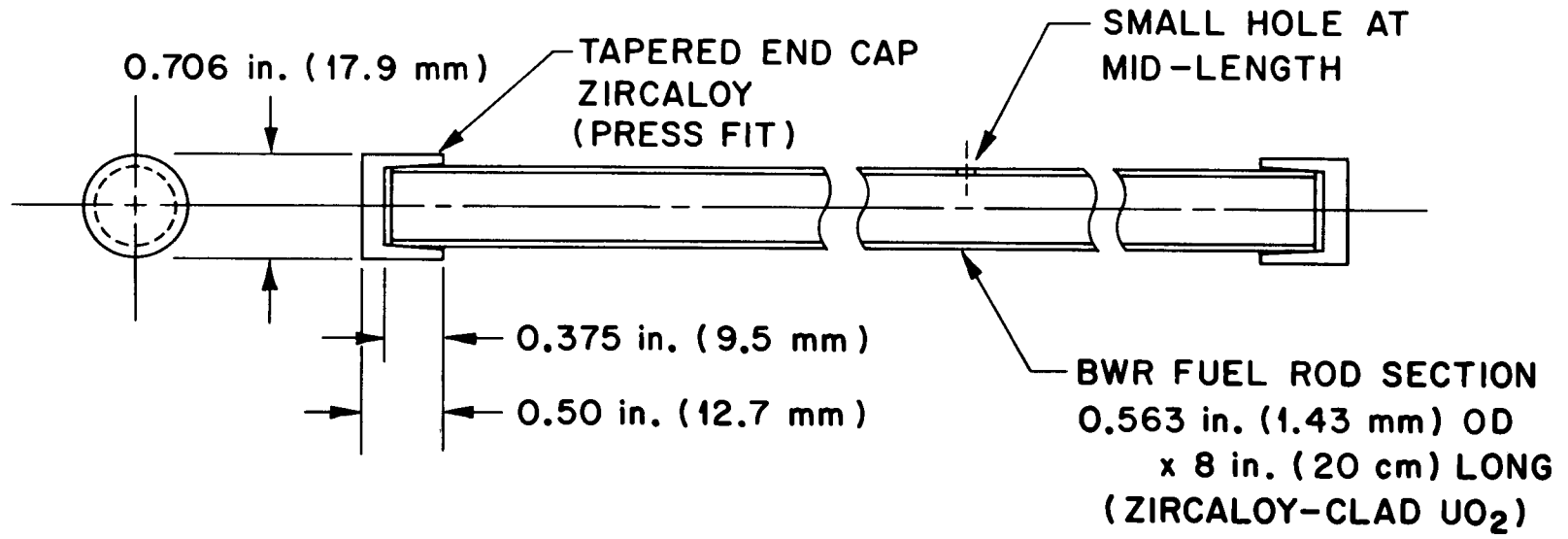


Fig. 2. Fuel specimen for fission product release studies.

Table 4. Analysis of gas removed from plenum and void spaces of Peach Bottom-2 fuel rod DG-2986

Component	Fraction of total (mol %)	Volume ^a (cm ³ , STP)	Volume ^b (cm ³ , STP)
H ₂	<0.1	<0.2	<0.2
He	43.6	79.1	79.1
N ₂	0.1	0.2	0.2
O ₂	<0.1	<0.2	<0.2
Ar	1.1	2.0	2.0
CO ₂	<0.1	<0.2	<0.2
Kr	5.4	9.8	9.68
Xe	49.7	90.2	90.2
Total			181.4 ± 1.8

^a Rod void volume measured at 74.0 ± 1.0 cm³ in January 1979.

^b Calculated amounts as of July 15, 1981.

Table 5. Fission gas found in the plenum of Peach Bottom-2 rod DG-2986

Isotope	Amount found in plenum ^a			Total produced; ORIGEN calculation ^c (mmol/kg)	Fraction of calculated yield found in the plenum (%)
	Fraction of element yield ^b (%)	[cm ³ (STP)]	(mmol/kg)		
⁸³ Kr	13.11	1.269	0.0141	0.156	9.044
⁸⁴ Kr	30.04	2.907	0.0324	0.345	9.405
⁸⁵ Kr	4.97	0.481	0.0054	0.055	9.908
⁸⁶ Kr	51.88	5.021	0.0559	0.587	9.517
Total Kr		9.678	0.1078	1.142	9.437
¹²⁸ Xe	0.02	0.018	0.0002	0.004	5.556
¹³⁰ Xe	0.10	0.090	0.0010	0.014	6.944
¹³¹ Xe	9.84	8.871	0.0988	1.141	8.661
¹³² Xe	19.09	17.21	0.192	2.163	8.863
¹³⁴ Xe	28.11	25.34	0.282	3.079	9.166
¹³⁶ Xe	42.84	38.62	0.430	4.654	9.242
Total Xe		90.16	1.004	11.05	9.083
Total Xe + Kr		99.83	1.112	12.2	9.116

^aQuantities calculated for 1937-d decay period (to July 15, 1981).

^bPercentages determined by EG&G Idaho, Inc.¹²

^cCalculated for 8.388 MWd/kg by linear decrease from an ORIGEN computer inventory calculation for 10.10-MWd/kg burnup.

ORNL DWG 79-901

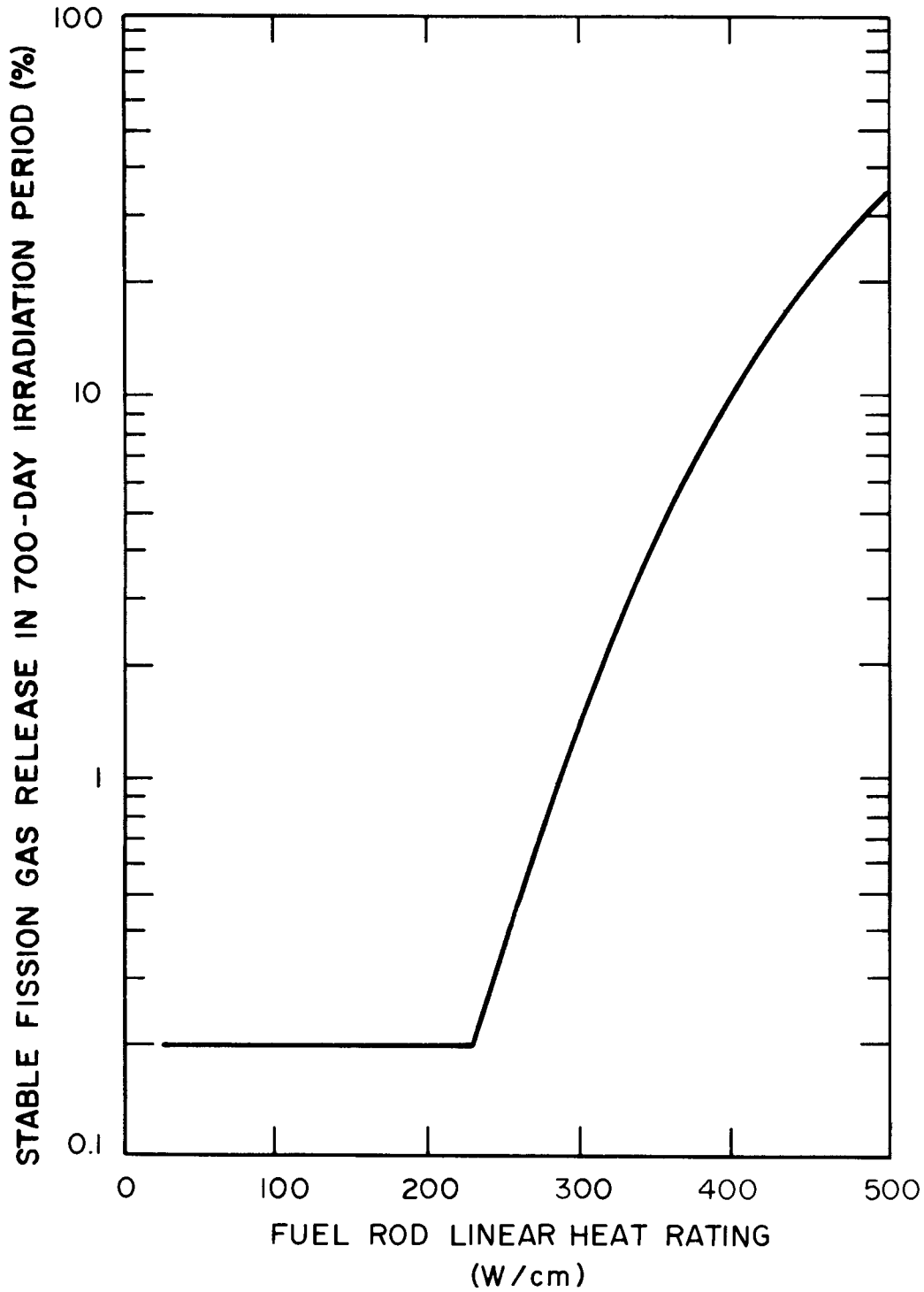


Fig. 3. Stable fission gas release estimated as a function of linear heat rating. (Source: ref. 13).

Table 6. Axial distribution of burnup and fission gas release for Peach Bottom-2 reactor fuel

Segment No.	Relative burnup ^a	Estimated burnup (MWd/kg)	Estimated fission gas released	
			(% of segment inventory)	(% of total rod inventory)
1	0.395	3.305	0.2	0.008
2	0.870	7.460	1.1	0.081
3 ^b	1.152	9.644	7.3	0.752
4 ^b	1.293	10.83	15.4	1.752
5 ^b	1.319	11.04	17.8	2.094
6 ^b	1.259	10.55	13.4	1.507
7	1.207	10.10	9.9 ^c	1.067
8	1.207	10.10	9.9 ^c	1.067
9	1.041	8.718	3.8	0.349
10	1.050	8.794	4.0	0.349
11	0.785	6.568	0.5	0.028
12	0.424	3.543	0.2	0.008
Rod av	1.000	8.388		9.116

^aObtained from gamma scan.

^bGamma scan indicated small peaks of activity between some pellets.

^cApproximately 10.2% Kr and 9.86% Xe.

at the correlation heat rating of ~ 440 W/cm and that the other segments experienced proportionally lower heat ratings. The calculated gas releases are listed in column 4 of Table 6 and were obtained by using the data in Fig. 3. Using the estimated burnup for a segment, the percentage of the total fission gas released from the segment was calculated. These values are listed in column 5 of Table 6.

The actual linear power varied considerably with time because of reactor power changes. Estimates of the peak heat rating and variations with time could be made by using the following information. Our examination of the daily power changes indicated that the reactor power was >500 MW for 652 d, >1000 MW for 536 d, >2500 MW for 365 d, and >3200 MW for 187 d. The total effective full-power days of operation were ~ 429 . For segment 5 (11.04 MWd/kg), the peak linear heat rating was 332 W/cm (10.2 kW/ft), based on the number of effective full-power days and averaged over the entire core-1 operation. Axial and radial flux pattern changes during the core-1 lifetime probably resulted in significant variation of the above-peak heat rating at full reactor power. We could not easily determine the magnitude of these variations from the relative neutron flux data presented in ref. 10. We believe that our inability to reconstruct the detailed axial power history of the test fuel rod does not seriously compromise the method used for estimating the fission gas release from each fuel rod segment since only relative release values are determined.

2.3 EXPERIMENTAL APPARATUS

The fuel specimen was heated in an induction furnace, as illustrated in Fig. 4. This furnace was developed from designs used in previous experimental efforts: fission product release tests,²⁻⁴ fuel rod burst experiments,⁷ and molten fuel tests.¹⁵ As in test HI-3, a graphite susceptor was used. It was protected by a blanket of helium gas. The furnace was mounted inside a stainless steel containment box in a hot cell, as shown in Figs. 5 and 6. The fission product collection system (Fig. 7) included a platinum thermal gradient tube, fiberglass filters, heated charcoal (for iodine adsorption), and cooled charcoal (for inert fission gas adsorption). The steam was collected in a condenser and a dryer, as indicated, prior to reaching the cooled charcoal. Instrumentation included two thermocouples (W-5% Re vs W-26% Re in a ZrO_2 tube) and an optical pyrometer for temperature measurement, NaI(Tl) radiation detectors connected to a multichannel analyzer, and conventional electrical and gas flow instruments. A data acquisition system (Fig. 8) was used to record test data at 1-min intervals, and several individual chart recorders maintained continuous records of temperatures and flow rates. Differences in apparatus materials and conditions for this test, compared with the previous tests, are summarized in Table 7.

2.4 TEST CONDITIONS AND OPERATION

The test was conducted under the operating conditions listed in Table 8. As in each of the previous experiments, the experimental apparatus was assembled by direct handling. This is possible because the hot-cell and test apparatus are decontaminated after each test. Also, a new

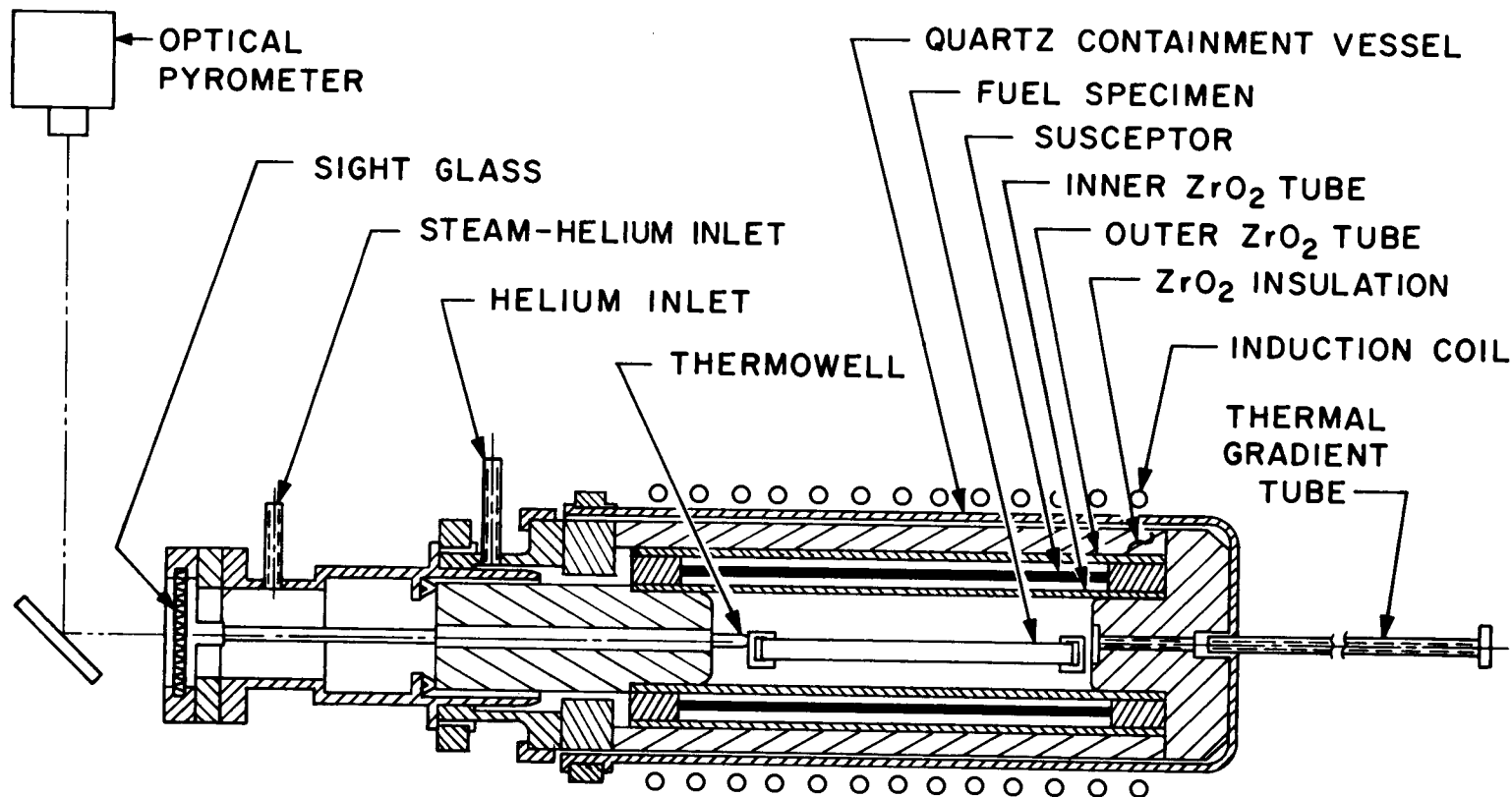


Fig. 4. Fission product release furnace.

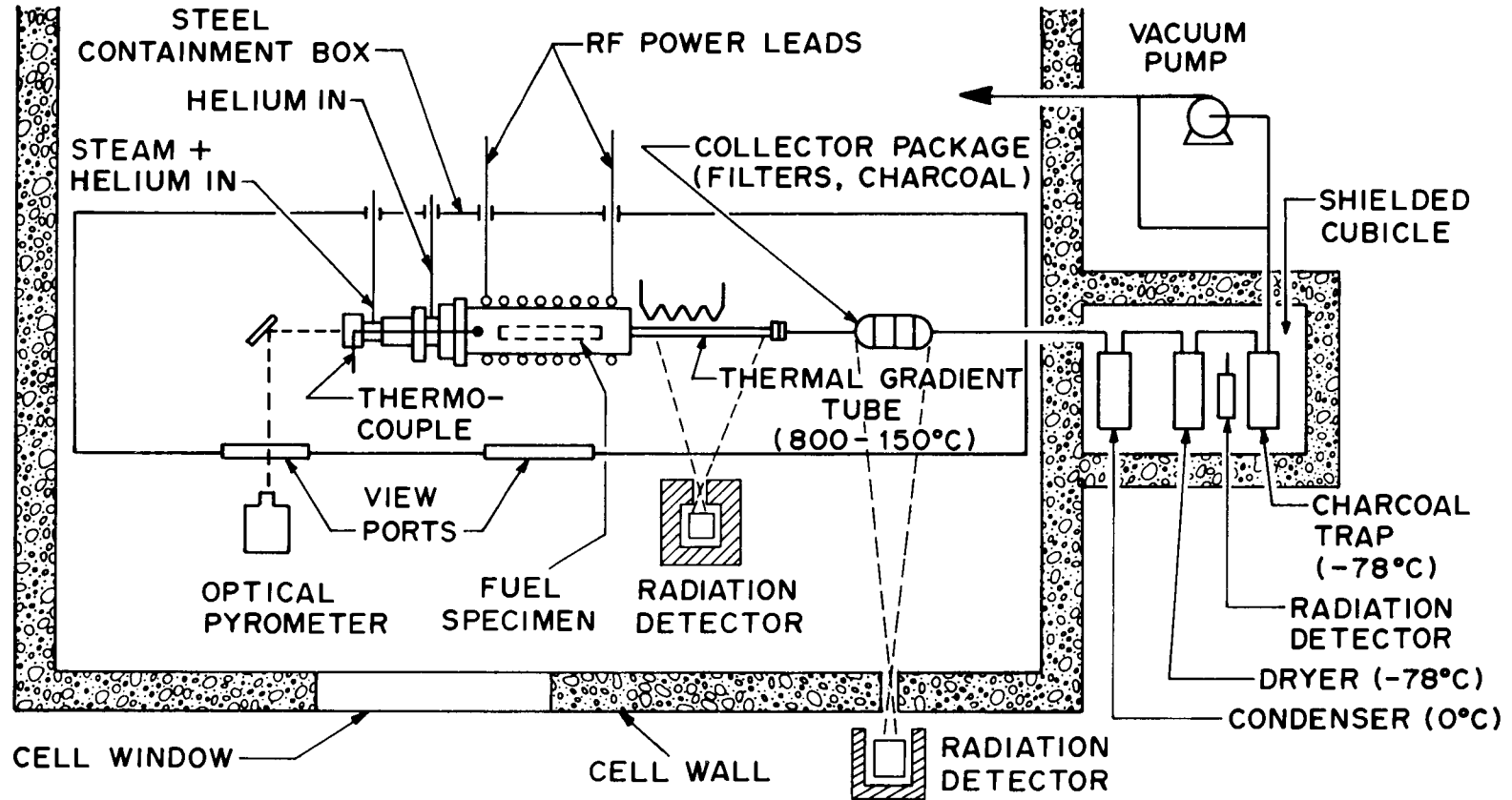


Fig. 5. Fission product release and collection system.

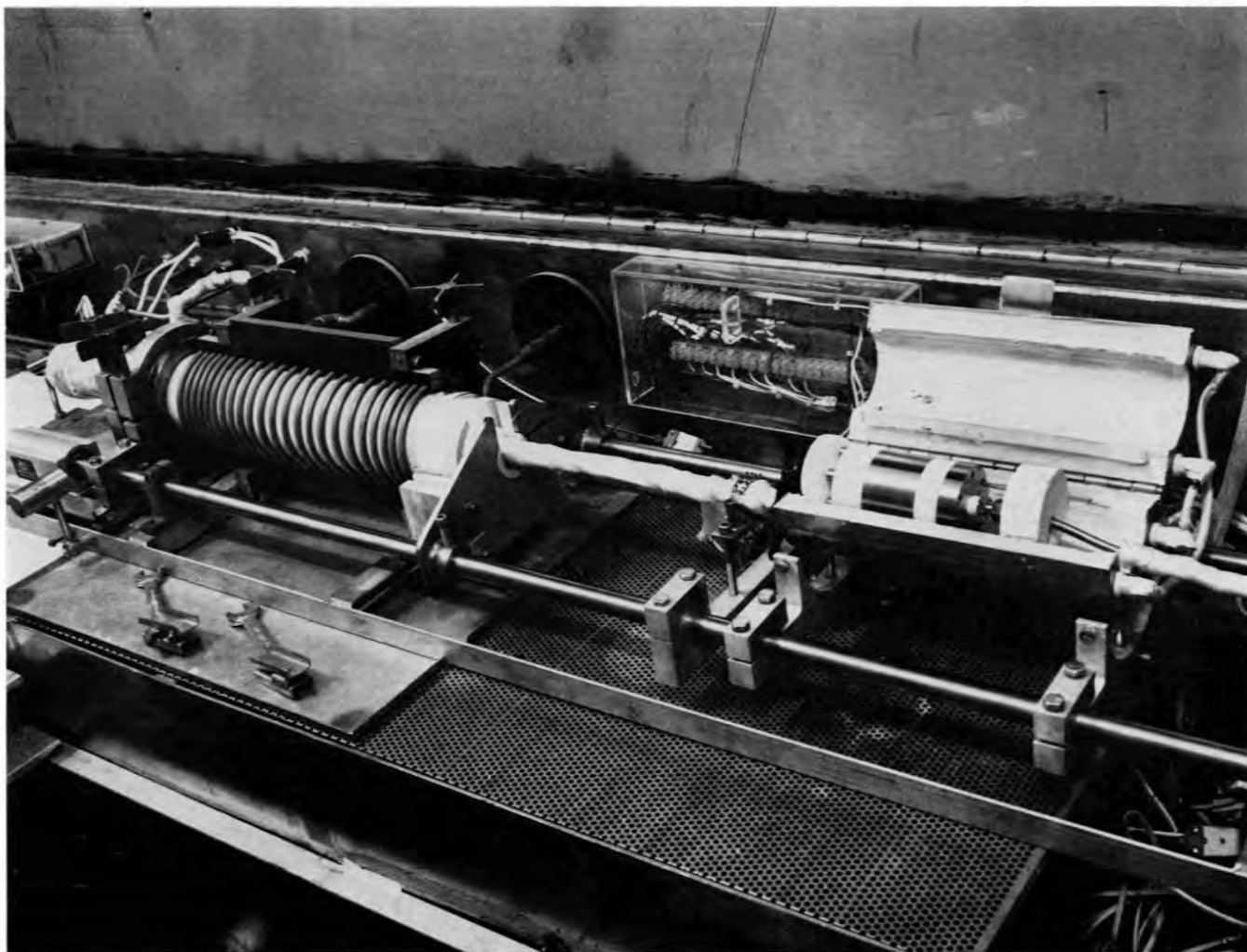


Fig. 6. Photograph of (a) fission product release furnace, (b) thermal gradient tube, and (c) filter package in steel containment box before test HI-2.

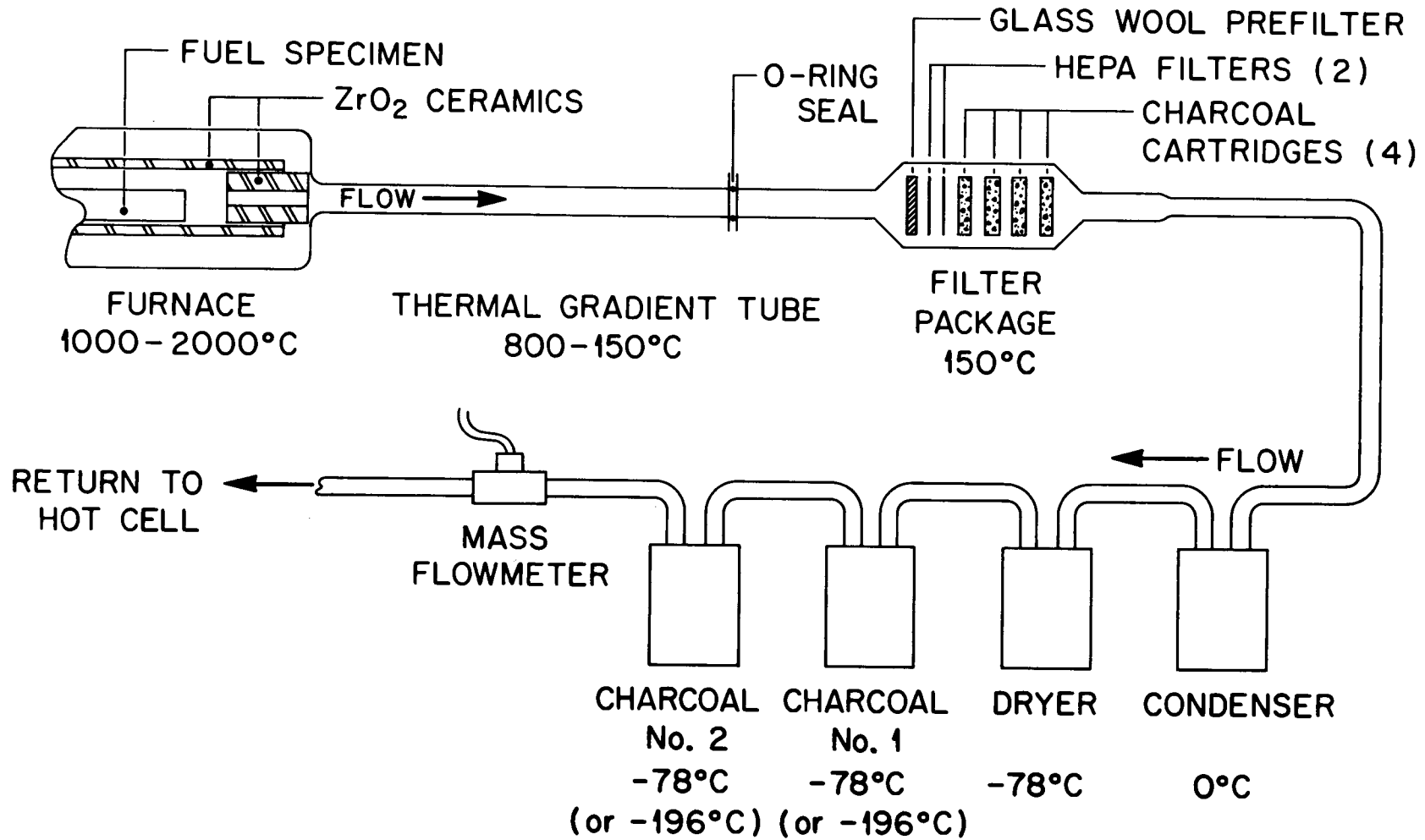


Fig. 7. Fission product collection system.

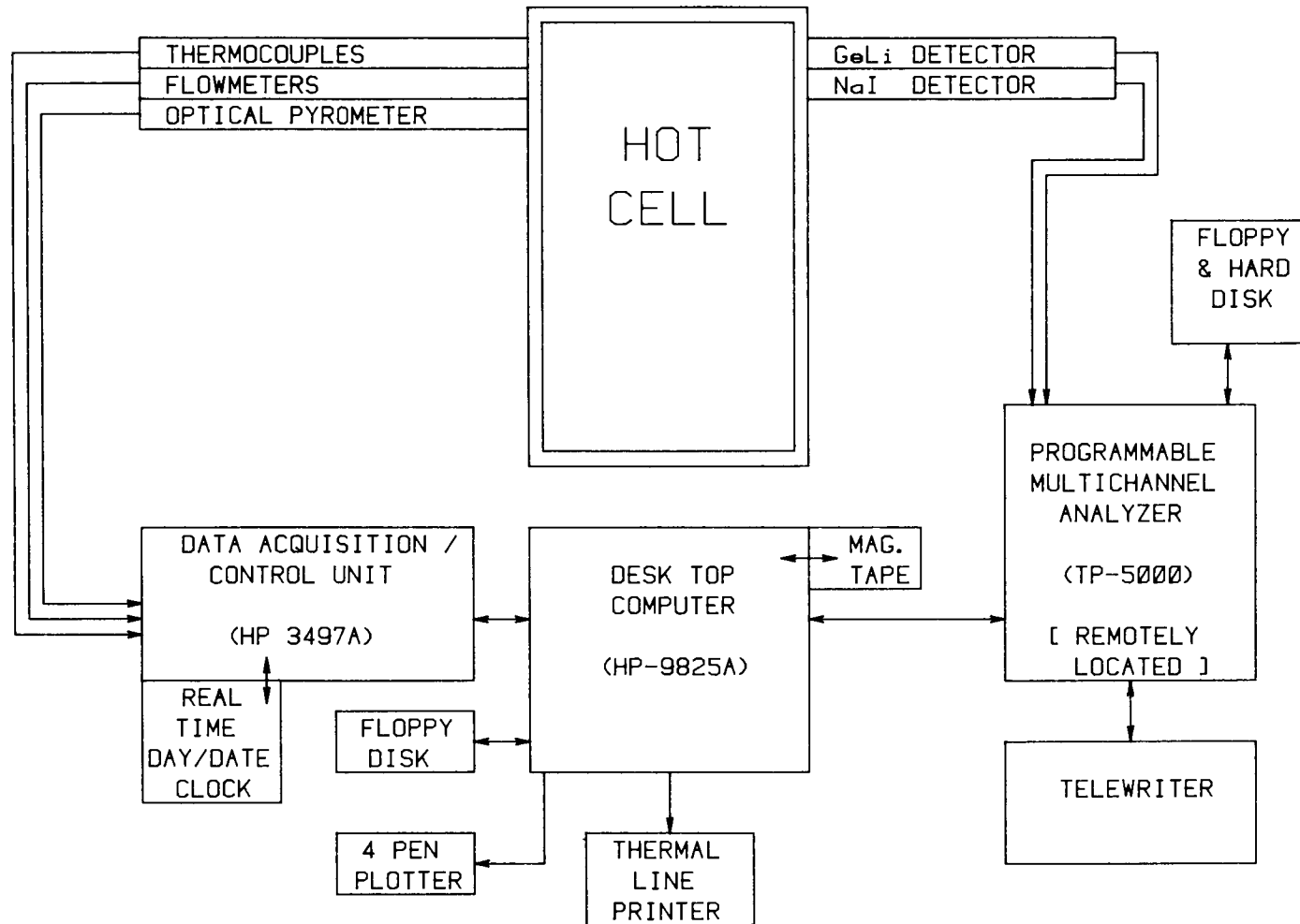


Fig. 8. Data acquisition and processing system for fission product release test.

Table 7. Comparison of apparatus and test conditions for the four HI tests

Component/condition	Test			
	HI-1	HI-2	HI-3	HI-4
Furnace thermocouple	Pt-10% Rh vs Pt (bare)	Pt-10% Rh vs Pt (bare)	W-5% Re vs W-26% Re (ZrO ₂ thermowell)	W-5% Re vs W-26% Re (ZrO ₂ thermowell)
Susceptor	Tungsten	Tungsten	Graphite	Graphite
Pretreatment of: Fibrous ZrO ₂ insulator	None	Zirconyl nitrate (one coat) + 1 h in air at 1000°C	Zirconyl nitrate (one coat) + 1 h in air at 1000°C	Zirconyl nitrate (two coats) + 1 h in air at 1000°C
High-density ZrO ₂ pieces	None	None	1 h in air at 1000°C	1 h in air at 1000°C
Thermal gradient tube liner	Platinum	Platinum/gold	Platinum	Platinum
Thermal gradient tube length, cm	30.5	35.6	35.6	35.6
Connector, thermal gradient tube to filter pack	3.2 mm ID × 76 mm long; Teflon	3.2 mm ID × 76 mm long; Teflon	4.6 mm ID × 190 mm long; stainless steel	4.6 mm ID × 190 mm long; stainless steel
Entrance cone to filter pack	Teflon	Teflon	Stainless steel	Stainless steel
Glass wool prefilter	30 mm diam; Teflon screen	30 mm diam; Teflon screen	51 mm diam; stainless steel screen	51 mm diam; stainless steel screen
Dryer and cold charcoal temperature, °C	-78	-78	-195	-195
Carrier gas	Argon	Argon	Helium	Helium + 0.05% H ₂

Table 8. Operating conditions for test HI-4

Heatup rate ^a	137°C/min
Nominal test temperature	1800°C ± 50
Time at test temperature	20 min
Flow rate data: ^b	
He purge to graphite susceptor	0.15 L/min
He to steam generator	0.15 L/min
Steam into system	0.32 L/min
Total flow data: ^c	
He purge	7.72 L
He to steam generator ^d	7.26 L
H ₂ generated ^e	13.66 L

^aPrior to rapid heatup, the specimen was heated to ~158°C to prevent steam condensation in the furnace tube when the steam flow was started.

^bAs measured by mass flowmeters.

^cAs measured by totalizers on mass flowmeters during the 50 min of steam flow into apparatus, operating at room temperature = 23°C.

^dAbsolute pressure in furnace during test was 0.1040 MPa (780 mm Hg).

^eAt atm = 0.0988 MPa (741.1 mm Hg). Hydrogen is produced by the reaction of steam with the Zircaloy cladding to form ZrO₂.

furnace tube assembly is used in each test. Transfer and loading of the highly radioactive fuel specimen and final closure of the furnace and containment box required the use of master slave manipulators. Once the hot cell was closed and sealed, no in-cell operations were required while testing. Prior to testing and before the steam flow was begun, the furnace was preheated to $\sim 300^{\circ}\text{C}$ and purged with helium. Also, all connecting lines to the furnace-thermal gradient tube-filter pack assemblies were preheated to at least 125°C to prevent steam condensation during the test.

Approximately 3 min after the test temperature (1850°C) was reached, a break developed in the ZrO_2 thermowell that housed the W-5% Re vs W-26% Re thermocouple. This caused some concern that the thermocouples might fail from rapid steam oxidation. This was not the case. The flow of helium through the thermowell appeared to minimize the exposure of the thermocouples to the steam, and they functioned well. The optical pyrometer also functioned well and showed that the inlet end of the fuel specimen was maintained at a temperature of $\sim 1850^{\circ}\text{C}$.

2.5 POSTTEST DISASSEMBLY AND SAMPLE COLLECTION

After the test was completed, the apparatus was disassembled. The filter assembly and the liner of the thermal gradient tube were removed and transferred to another hot cell to avoid potential contamination from fuel handling. As in test HI-3,⁸ the oxidized cladding appeared to have puffed up during the test and the fuel specimen could not be removed from the ZrO_2 furnace tube. Furthermore, the inlet zirconia spacer was also frozen to the same tube. Apparently there was enough cladding melting and/or reaction with the ZrO_2 boat and furnace tube liner to cause these components to be fused together. (This explanation is plausible because the melting point of Zircaloy-4 is reported to be $\sim 1760^{\circ}\text{C}$.¹⁶) Both the inlet and outlet end caps were clearly visible. The inlet end cap was white and flaky, which suggests heavy oxidation. The outlet end cap appeared unchanged. Since the steam flow rate was low during the test, this was not surprising. The test period (20 min) was not long enough to allow complete oxidation of the specimen; therefore, the outlet end was under a reducing hydrogen blanket during the test. Gas flow data indicated that the cladding was $\sim 54\%$ oxidized, based on the amount of steam that reacted with the cladding.

As in test HI-3, the entire ZrO_2 furnace tube liner containing the fused fuel specimen and inlet ZrO_2 spacer had to be placed in a glass tube and cast in epoxy resin to preserve the relative sample integrity during handling and transfer to another hot cell. This assembly was analyzed for radioactive fission product content by gamma spectrometry. It was also gamma-scanned at 1-cm intervals to determine fission product distribution along the specimen. These data were compared with pretest data (Sect. 3.2.7). The fuel specimen was then transferred to the High Radiation Level Examination Laboratory, where it was cut into radial sections for detailed inspection (Sect. 3.2.6). After the highly radioactive test components were removed from the hot cell, the cell was decontaminated. Gamma-ray analyses were carried out on all test components.

The thermal gradient tube liner and the quartz wool filter were weighed before and after the test to determine any weight change. The measurements showed a gain of 0.03 and 0.07 g, respectively, during the test.

Because of the high level of radioactivity, the platinum thermal gradient tube liner had to be gamma-ray counted through 2.54 cm of lead. It was also gamma-scanned at 1.0-cm intervals to determine the distribution of radioactivity (primarily ^{137}Cs) with temperature (see Sect. 3.2.4). Subsequently, the thermal gradient tube was cut into ten sections and gamma counted. A graphite electrode smear sample of each of these sections was taken for spark-source mass spectrometric (SSMS) analysis.

Each section of the thermal gradient tube liner and component of the filter assembly was analyzed by gamma spectrometry, before and after leaching successively with basic ($\text{NH}_4\text{OH} + \text{H}_2\text{O}_2$) and acidic ($\text{HNO}_3 + \text{HF}$) solutions. The quartz furnace vessel, the quartz thermal gradient tube housing, and a few of the furnace outlet end ceramic components were also leached in a similar fashion. Iodine release values were obtained by neutron activation analysis of the leach solutions and of the charcoal from the filter assembly.

3. TEST RESULTS

3.1 TEST DATA

The temperature and flow history of the entire test is presented in Fig. 9. These are uncorrected data; posttest temperature calibrations showed that the temperature as indicated by the optical pyrometer was $\sim 150^\circ\text{C}$ lower than the actual temperature at the inlet end of the 8-in. fuel rod segment. This agrees with previous calibrations of the optical pyrometer. There was also a temperature gradient of $\sim 100^\circ\text{C}$ from the inlet to the outlet ends of the segment. Figure 10 shows an estimated temperature profile that is based on the posttest calibrations and metallographic data. Test operating conditions are summarized in Table 8. As mentioned in Sect. 2.5, we estimate that 54% of the Zircaloy-4 cladding was oxidized. The release histories of ^{85}Kr to the cold charcoal traps and of the ^{137}Cs to the thermal gradient tube and the filters as related to test time and temperature are shown in Fig. 11. These values were determined as relative rates during the test. Quantitative measurements were made with a multichannel analyzer to determine the actual fractional releases. The detector for the thermal gradient tube was positioned at a point where only the lower-temperature end of the tube could be viewed. As indicated by the release curves, a significant release occurred during the rapid cooling of the specimen after the induction power supply was turned off. This was probably caused by cracks developing in the pellets and oxidized cladding.

3.2 POSTTEST DATA

Gamma-ray spectrometric analysis of the disassembled apparatus components revealed that the principal radioactive species present were ^{137}Cs

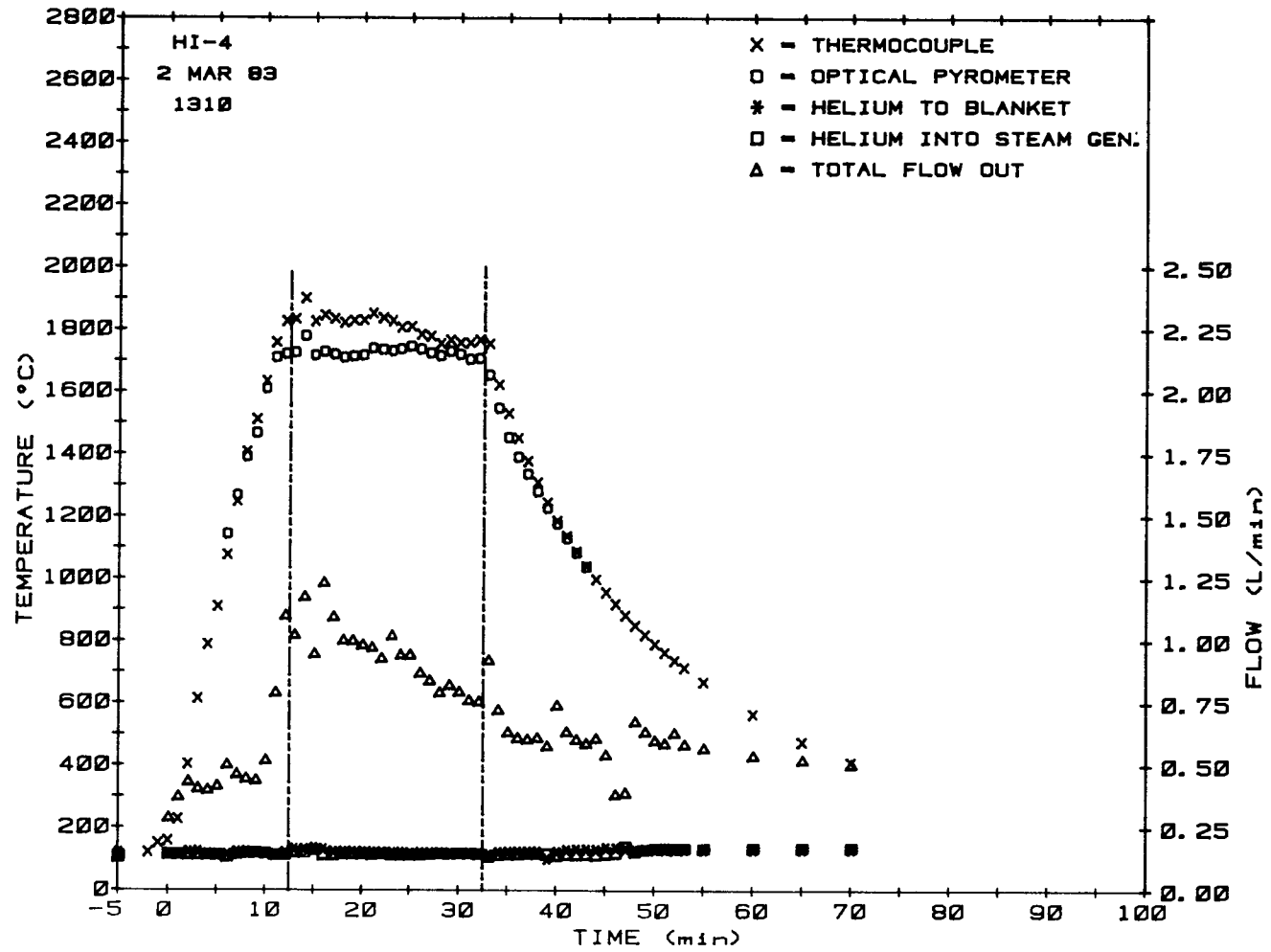


Fig. 9. Temperature and flow history of test HI-4.

ORNL DWG 83-987

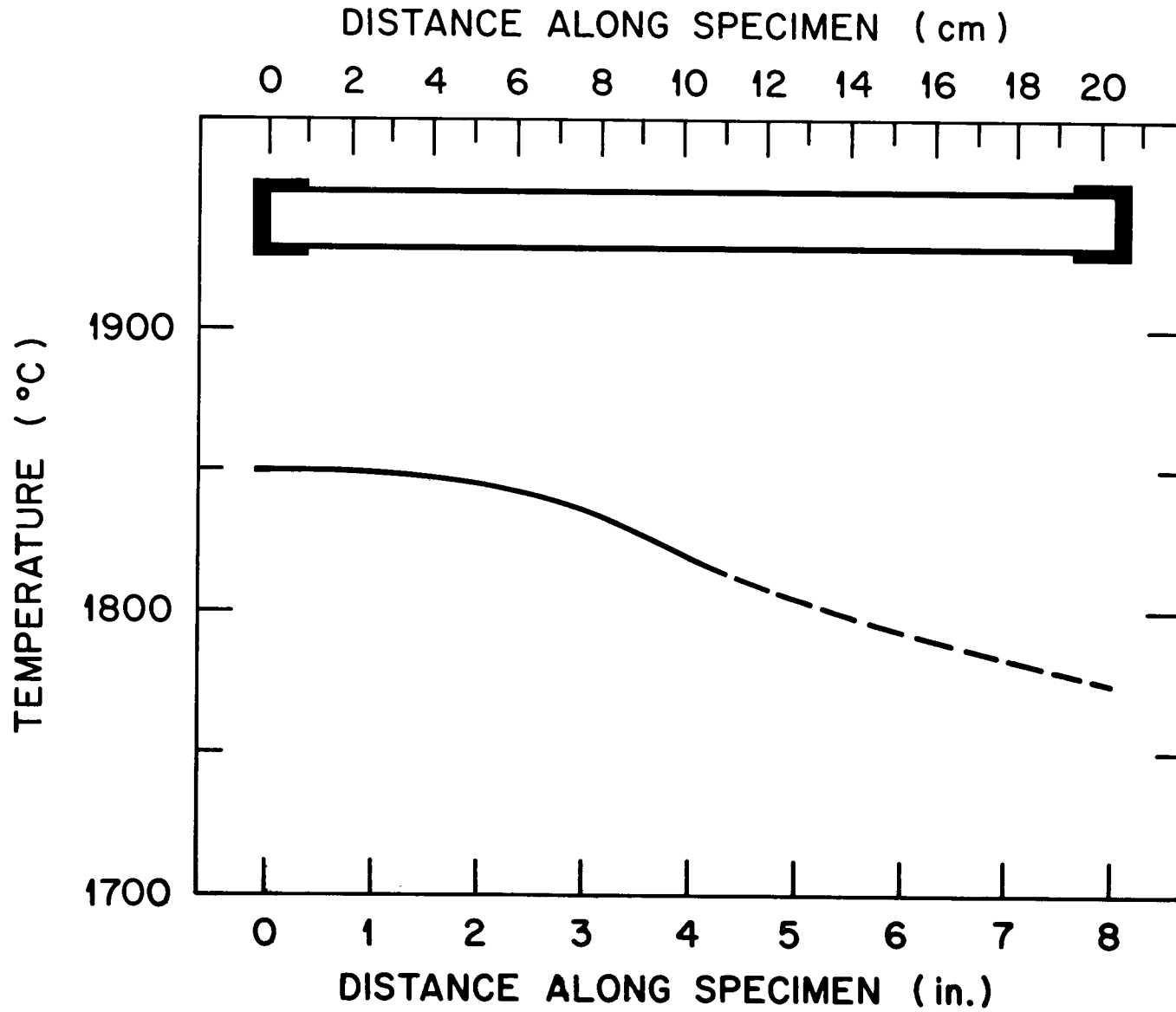


Fig. 10. Estimated temperature profile of fuel rod segment during test HI-4.

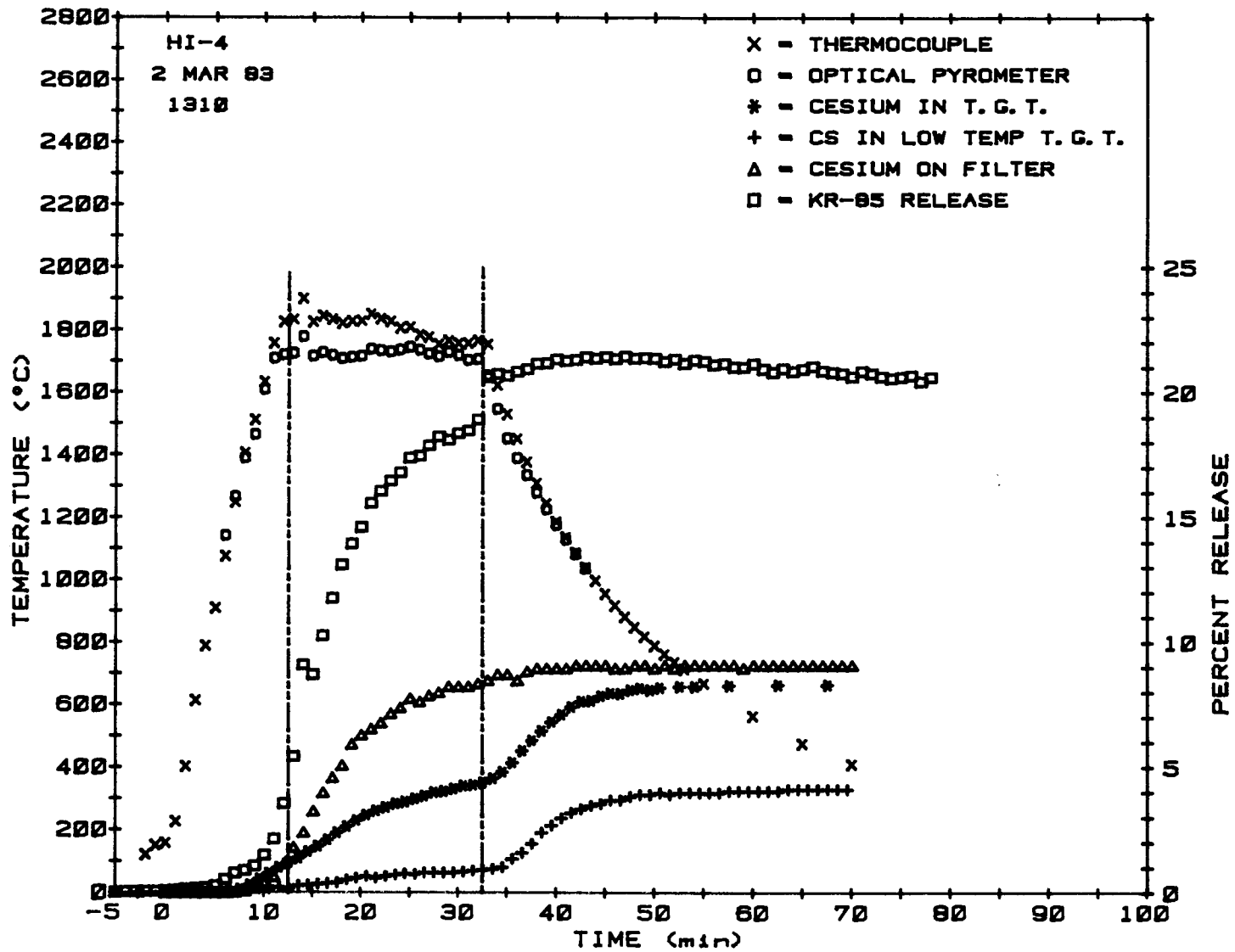


Fig. 11. Collections of ^{85}Kr and ^{137}Cs as functions of temperature and time in test HI-4.

and ^{134}Cs . Unfortunately, the high level of cesium activity interfered with the analysis of less abundant fission products. A summary of the fractional release results for the various system components, as determined by gamma spectrometry and activation analysis, is presented in Table 9. Note that the krypton and cesium releases are almost identical, 31.3 and 31.7% of calculated segment inventories, respectively. The krypton value includes an estimated 10.2% (see Table 6) of the segment inventory which was released to the pellet-clad gap during irradiation. This gas, which was released to the gap during irradiation, was collected and analyzed prior to the parent fuel rod being cut into segments.

Table 9. Distribution and fractional release of fission products in test HI-4

Test component or collector	Temperature or range (°C)	Fraction of fission product inventory found (%)				
		^{85}Kr	^{137}Cs	^{129}I	^{125}Sb	$^{110\text{m}}\text{Ag}$
Furnace	1850-1000	0	14.13	0.89	>0.0086	>0.023
Thermal gradient tube	900-140	0	8.49	8.56	>0	>0.071
Filters	125	0	9.10	15.20	0	0
Hot charcoal	125	0	10^{-4}	10^{-3}	0	0
Cold charcoal	-196	21.13	0	0	0	0
Total		21.13 ^a	31.72	24.65	>0.0086	>0.094

^aIt is estimated that 10.2% of the segment inventory of ^{85}Kr was released to the pellet-cladding gap during irradiation (see Table 6). The total ^{85}Kr release would have been ~31.33% if that gas had been available in the test specimen.

The apparent release of antimony was low, $8.6 \times 10^{-2}\%$, because (1) the cladding was not completely oxidized and (2) the cesium radioactivity caused high limits of detection for antimony. Antimony reacts with unoxidized Zircaloy, thereby lowering the release rate from the furnace. The released antimony was found on component surfaces near the inlet end of the test specimen. Posttest examination of the test specimen revealed that only the inlet end was completely oxidized.

3.2.1 Results from Gamma Spectrometry

Table 10 provides the detailed results of gamma spectrometric analysis for ^{137}Cs . Approximately 45% of the released cesium remained in the

Table 10. Distribution of cesium in test HI-4

Location	Temperature (°C)	Cesium found in each location			
		Amount ($\mu\text{Ci } ^{137}\text{Cs}$)	(mg total Cs)	Percentage of specimen inventory ^a	Percentage of released
Furnace components					
Inlet end components	~1000	1.098+2 ^b			
Outer ZrO ₂ tube	~1850	4.432+2			
Fibrous ZrO ₂ insulator	900-1700	5.186+2			
Graphite susceptor	~2000	4.233+2			
Outlet end components	900-1400	1.801+5			
ZrO ₂ outlet end plugs	900-1700	6.714+5			
Miscellaneous debris	900-1800	1.129+4			
Quartz vessel	~800	9.546+4			
Total		1.002+6	29.09	14.13	44.56
Thermal gradient tube^c					
Quartz tube	837-197	1.834+4			
Pt segment 1	837-577	2.041+4			
Pt segment 2	737-447	1.602+5			
Pt segment 3	697-447	5.450+4			
Pt segment 4	637-497	4.762+4			
Pt segment 5	547-467	4.375+4			
Pt segment 6	487-387	8.247+4			
Pt segment 7	387-317	7.990+4			
Pt segment 8	317-267	4.433+4			
Pt segment 9	267-227	3.353+4			
Pt segment 10	227-197	1.660+4			
Wipe from push rod		2.462+2			
Total		6.019+5	17.48	8.49	26.77
Filter package					
	140				
Entrance tube		1.400+4			
Entrance cone		1.775+2			
Glass wool prefilter		5.991+5			
First HEPA filter		2.941+4			
Second HEPA filter		8.669+1			
Heated charcoal		4.286-4			
Miscellaneous parts		2.052+3			
Total		6.448+5	18.72	9.10	28.67
Other components					
Condenser	0				
Dryer	-196				
Cooled charcoal	-196				
Total					
Total all components		2.249+6	65.29	31.72	100

^aBased on average burnup of 10.1 MWd/kg, the test specimen contained 205.83 mg of cesium and 7.089 Ci of ¹³⁷Cs (= 2.903E-5 mg Cs/ $\mu\text{Ci } ^{137}\text{Cs}$); decay corrected to July 15, 1981 (ORIGEN calculation).

^bExponential notation: 1.098+2 = 1.098 × 10², etc.

^cTemperature ranges overlap because heater No. 2 for the thermal gradient tube burned out.

furnace tube at the outlet end. Of the ^{137}Cs that escaped the furnace, about half deposited on the platinum thermal gradient tube liner and the other half on the filters (mainly on the glass wool). The distribution of cesium throughout the test apparatus is illustrated in Fig. 12; the iodine distribution, as determined by component leaching and activation analysis for ^{129}I , is shown for comparison. About 13.2 times more cesium was released than iodine. According to ORIGEN (see Table 2), there was 10.3 times more cesium in the fuel rod segment than iodine. The largest concentrations of cesium were found on the zirconia outlet end plug and the glass wool prefilter. The deposit on the 4-cm-long plug indicates a possible reaction (perhaps the formation of cesium zirconate). It was also determined that ~93% of the cesium was on the outlet half. The cesium on the filter probably was transported there as an aerosol.

3.2.2 Results of Activation Analysis for Iodine

Since iodine has no long-lived, gamma-emitting nuclides, analytical methods other than gamma spectrometry must be used. Neutron activation of ^{129}I to ^{130}I ($t_{1/2} = 12.4$ h), which can be counted easily, is a proven, sensitive technique. Iodine forms dissolve readily in basic solutions to form stable iodides; in our samples, large amounts of highly radioactive cesium were also dissolved. Small aliquots of the solutions were chemically treated to remove cesium, irradiated, and counted for ^{130}I . The results of these analyses, along with data for fractional iodine release and cesium/iodine ratios at various apparatus locations, are summarized in Table 11. The total fraction of iodine released was 24.7%, a minimum value. Since iodine cannot be detected directly, it has to be leached from the surfaces of the components as discussed above. With this procedure, there is always some uncertainty about the iodine being completely removed by the leaching steps. Approximately 62% of the detected iodine was found in the filter pack, mostly on the glass wool filter. Iodine that collected on the glass wool filter probably was transported there by particulate material or as an aerosol. Very small amounts of the iodine (~0.01%) were collected on the second HEPA filter and the heated charcoal. Only the most volatile and penetrating forms of iodine, such as methyl iodide and elemental iodine, are expected to be collected beyond the glass wool and the first HEPA filters.

The heated charcoal was also analyzed for bromine by activation analysis. The results showed ~0.31 μg bromine, which corresponds to about $1.9 \times 10^{-2}\%$ of the specimen calculated inventory. Any bromine released from the test specimen would be expected to behave in a manner similar to that observed for iodine. It should be pointed out, however, that the specimen contained 123 times more Cs and 12 times more I than Br, according to the ORIGEN values in Table 2.

3.2.3 Results of SSMS Analysis

Elemental analyses were obtained by SSMS for graphite electrode smear samples at ten locations along the platinum thermal gradient tube and one from the glass wool filter. Following the sampling, the amount of ^{137}Cs in each sample was determined by gamma spectrometry. These values were

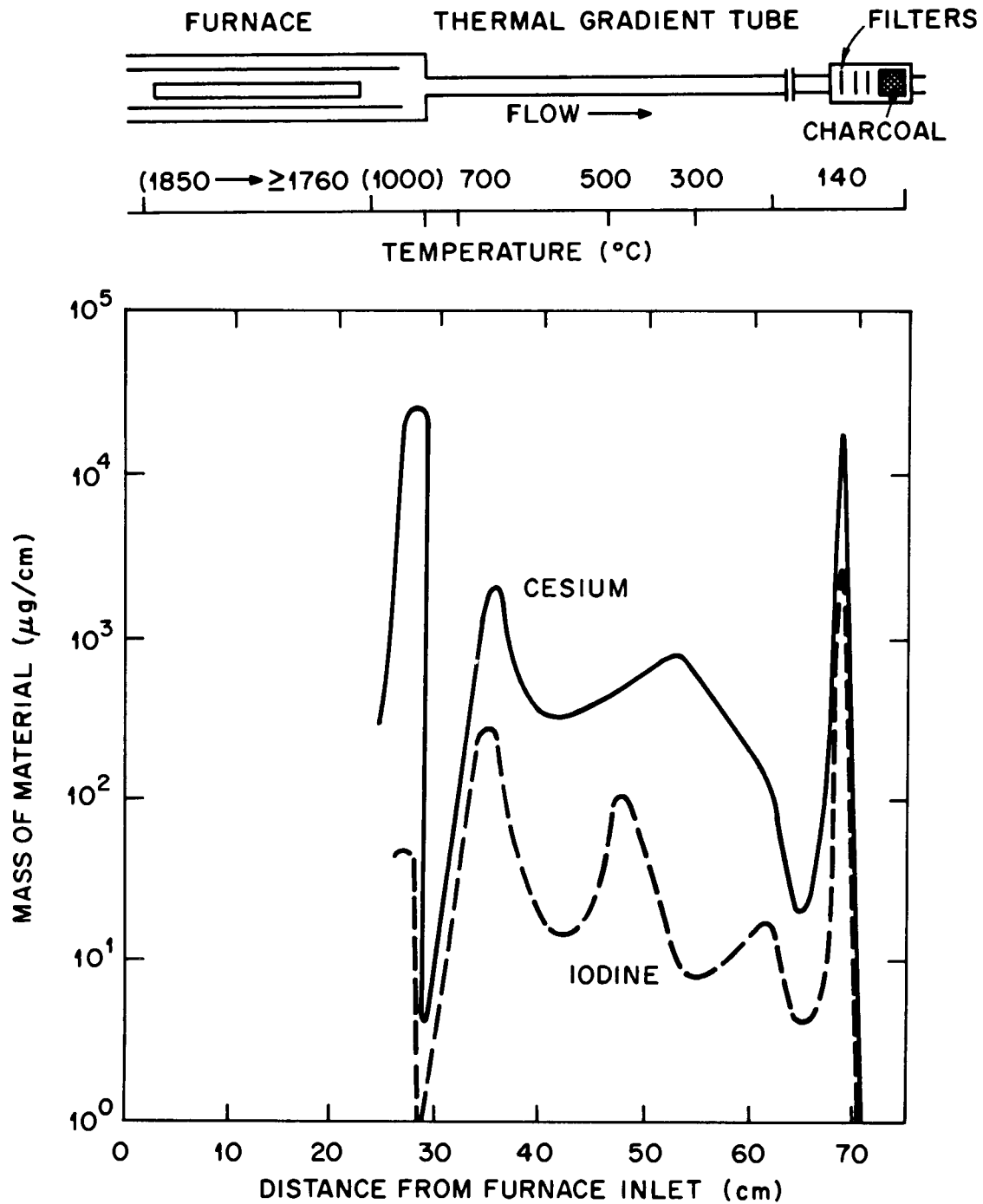


Fig. 12. Distribution of cesium and iodine in test HI-4.

Table 11. Fractional release and distribution of iodine in test HI-4
(results of activation analysis for ^{129}I)

Location	Temperature (°C)	Iodine found at each location		Percentage of specimen inventory ^a	Percentage of released	C/I ratio ($\mu\text{g Cs}/\mu\text{g I}$)
		Amount ($\mu\text{g }^{129}\text{I}$)	($\mu\text{g total I}$)			
Furnace components						
Quartz vessel	~800	20.43	26.95			102.8
ZrO ₂ outlet end plug	900-1200	113.91	150.28			129.7
Total ^b		134.34	177.23	0.89	3.60	125.6
Thermal gradient tube ^c						
Quartz tube (all)	837-197	32.84	43.32			12.3
Segment 1	837-577	70.57	93.10			6.4
Segment 2	737-447	563.85	743.87			6.3
Segment 3	697-447	140.45	185.30			8.5
Segment 4	637-497	49.24	64.96			21.3
Segment 5	547-467	88.32	116.52			10.9
Segment 6	487-387	222.46	293.48			8.2
Segment 7	387-317	39.84	52.56			44.1
Segment 8	317-267	19.18	25.30			50.9
Segment 9	267-227	27.83	36.71			26.5
Segment 10	227-197	43.18	56.96			8.5
Total		1297.76	1712.08	8.56	34.73	10.2
Filter package ~125						
Entrance tube		43.68	57.62			7.1
Entrance cone		0.59	0.78			6.6
Glass wool filter		2134.47	2815.92			6.2
First HEPA filter		122.12	161.11			5.3
Second HEPA filter		0.27	0.36			7.0
Charcoal ^d		0.21	0.28			4.4×10^{-5}
Miscellaneous parts		2.95	3.89			15.3
Total		2304.29	3039.98	15.20	61.67	6.2
Total all components		3736.39	4929.29	24.65	100.00	13.2

^aBased on an average burnup of 10.1 MWd/kg, the test specimen contained 15.6 mg of ^{129}I and 20.0 mg of total iodine; decay corrected to July 15, 1981.

^bSmall amounts of iodine probably were present on other furnace components that were not leached.

^cTemperature ranges overlap because heater No. 2 for the thermal gradient tube burned out.

^dIn addition, 0.31 μg of bromine was found on the charcoal; this value corresponds to 0.019% of the specimen inventory compared with 0.006% of the iodine found on the charcoal.

then used as the standards in determining mass values for the fission products, structural materials, and impurity elements that were detected on the samples.

Table 12 summarizes the results obtained by SSMS analysis. These data are divided into three groups: (1) fission products; (2) special materials, such as fuel (U) and cladding (Zr and Sn), and apparatus structural materials (Zr, Mg, Ca, and Pt); and (3) other materials (impurities in the system). The values for the thermal gradient tube were obtained by making the assumption that each sample was representative of all the deposited material in a 1-cm length of the thermal gradient tube at the sampling location (of course, this might not always be true). The SSMS results for a smear sample were multiplied by the detected amount of ^{137}Cs in the centimeter section (from gamma measurements) and divided by the known amount of ^{137}Cs in the smear sample from SSMS measurement. The data for the glass wool filter were treated in a similar fashion, but the SSMS values were multiplied by the total mass of ^{137}Cs on the filter. This method of analysis should be considered only semiquantitative in nature; however, it does provide information about those elements that are transported to the collection train but cannot be determined by gamma spectrometry or neutron activation analyses.

Selected data from Table 12 are plotted in Figs. 13-15 to illustrate the distribution along the thermal gradient tube. The profile for iodine in Fig. 13 shows that there were two major iodine peaks. The dashed-line plot for iodine was based on data from activation analysis of leach samples. The similarity in profile shapes and mass quantities adds confidence to both methods of measurement. It should be noted, as indicated in Table 12, that the percentage of fission products in the region of the downstream iodine peak is >90%. At the 15.2-cm location, 94% of the material found was cesium. In the absence of iodine and other anion elements, the primary species could be CsOH .

The distribution profile for cadmium in the thermal gradient tube is shown in Fig. 13. These data suggest that there is a total of ~2 mg cadmium. More cadmium than cesium was present at the 31.8-cm location.

The mass of aerosol that deposited on the glass wool filter was ~75.3 mg (Table 12), which is in excellent agreement with the value, 70 ± 5 mg, obtained by weighing the filter before and after the test. Only ~46% of the aerosol weight was fission product according to the SSMS results.

The value for iodine on the filter was 4 mg, as compared with 2.8 mg determined by neutron activation analysis. Interestingly, the ratio of cesium to rubidium is 6 and the ratio of iodine to bromine is 14, compared with ratios of 8 and 12 using the ORIGEN values in Table 2. When the uncertainties of the analysis are taken into consideration, the SSMS data in Table 11 are considered to be very good.

The amounts of radiogenic silver (1.4 mg) and cadmium (8.6 mg) on the filter are significant. They represent ~19 and 63% of the fuel specimen inventories of those fission products, respectively.

Table 12. Results of spark-source mass spectrometric analysis of samples from test HI-4

Element	Mass of element found										Filter-1 (mg total)
	Thermal gradient tube sample (mg/cm)										
	1	2	3	4	5	6	7	8	9	10	
Distance from inlet (cm)	0.3	4.9	8.1	11.1	15.2	18.4	22.5	25.0	28.4	31.8	
Fission products											
Cs(R) ^a	0.004	0.884	0.758	0.329	0.379	0.480	0.758	0.607	0.329	0.190	17.393
Cd(R)				0.041	0.009	0.095	0.153	0.028	0.058	0.257	8.563
I(R)		0.310	0.241	0.026	0.003	0.227	0.053	0.018	0.027	0.060	3.996
Rb(R)	1.5 × 10 ⁻⁵	0.110	0.050	0.020	0.005	0.047	0.038	0.042	0.135	0.180	2.855
Ag(R)									0.0008	0.0013	1.427
Br(R)		0.110	0.101	0.004		0.005	0.004	0.001	0.001	0.0013	0.285
Te								<0.0006		<0.0003	<0.143
Eu									<6 × 10 ⁻⁵	<0.0001	<0.057
La								<6 × 10 ⁻⁵	<6 × 10 ⁻⁶	<10 ⁻⁶	<0.017
Ba								<0.0001	<10 ⁻⁵	<4 × 10 ⁻⁵	<0.017
Sr									<4 × 10 ⁻⁶	<1 × 10 ⁻⁵	<0.003
Total	0.004	1.414	1.150	0.420	0.396	0.854	1.006	0.697	0.551	0.670	34.76
Special materials^b											
Sn(N)		<0.003	0.402						<0.0001		
Zr(N)				0.012	0.004	0.001	0.001	0.0008	0.0004	0.0012	
Mg	0.0025	0.332	0.502	0.020	0.002	0.002	0.153	0.028	0.097	0.115	19.982
Ca(N)		0.006	0.005	0.006	0.002	0.001	0.002	0.003	0.0002	0.001	0.285
Pt		1.107	0.502	0.406	0.023	0.189	0.305	0.564	0.097	0.128	<0.200
U								<0.0003	<0.0001	<0.001	<0.086
Total ^c	0.003	0.341	0.909	0.038	0.006	0.004	0.156	0.032	0.098	0.118	20.35
Other materials^d											
Cl	0.0005	0.110	0.201	0.061	0.003	0.014	0.031	0.014	0.010	0.010	8.564
S	0.0005	0.332	0.402	0.203	0.005	0.047	0.153	0.198	0.136	0.115	5.709
Na	0.00005	0.078	0.352	0.020	0.001	0.003	0.015	0.003	0.006	0.004	2.569
Zn	0.0003	0.022	0.402	0.142	0.002	0.003	0.002	0.003	0.002	0.005	1.427
Pb		0.006	0.015				0.002	0.002	0.002	0.001	0.856
K	0.00005	0.022	0.025	0.020	0.002	0.014	0.008	0.002	0.001	0.0008	0.285
Fe	0.0001	0.011	0.005	0.012	0.005	0.002	0.005	0.006	0.008	0.006	0.257
P	0.00003	0.003	0.005	0.002		0.0002	0.0003	0.0003	0.0004	0.0004	0.200
Mn	0.00002	<0.001	<0.001	<0.001			0.001	<0.0003	<6 × 10 ⁻⁵	0.0004	0.200
Cu										0.00013	0.057
Cr		<0.001		<0.001	<0.001	<0.0001		<0.0003		<9 × 10 ⁻⁵	<0.029
Bi			0.025					0.001			
Al	0.00005	0.004	0.002	0.004	0.0002	0.001	0.0006	0.002	0.0001	0.0009	
Total	0.0017	0.591	1.435	0.468	0.019	0.084	0.217	0.232	0.166	0.144	20.15
Total all materials	0.009	2.346	3.494	0.926	0.421	0.942	1.379	0.961	0.815	0.952	75.26
Percentage fission product											
	44.4	60.3	32.9	45.4	94.1	90.7	73.0	72.5	67.6	70.4	46.2

^a(R) denotes radiogenic isotopic distribution and (N) denotes natural isotopic distribution.
^bMaterial known to be part of test system, such as fuel, cladding, and apparatus materials.
^cExcluding platinum, the deposition surface.
^dApparently impurities in system.

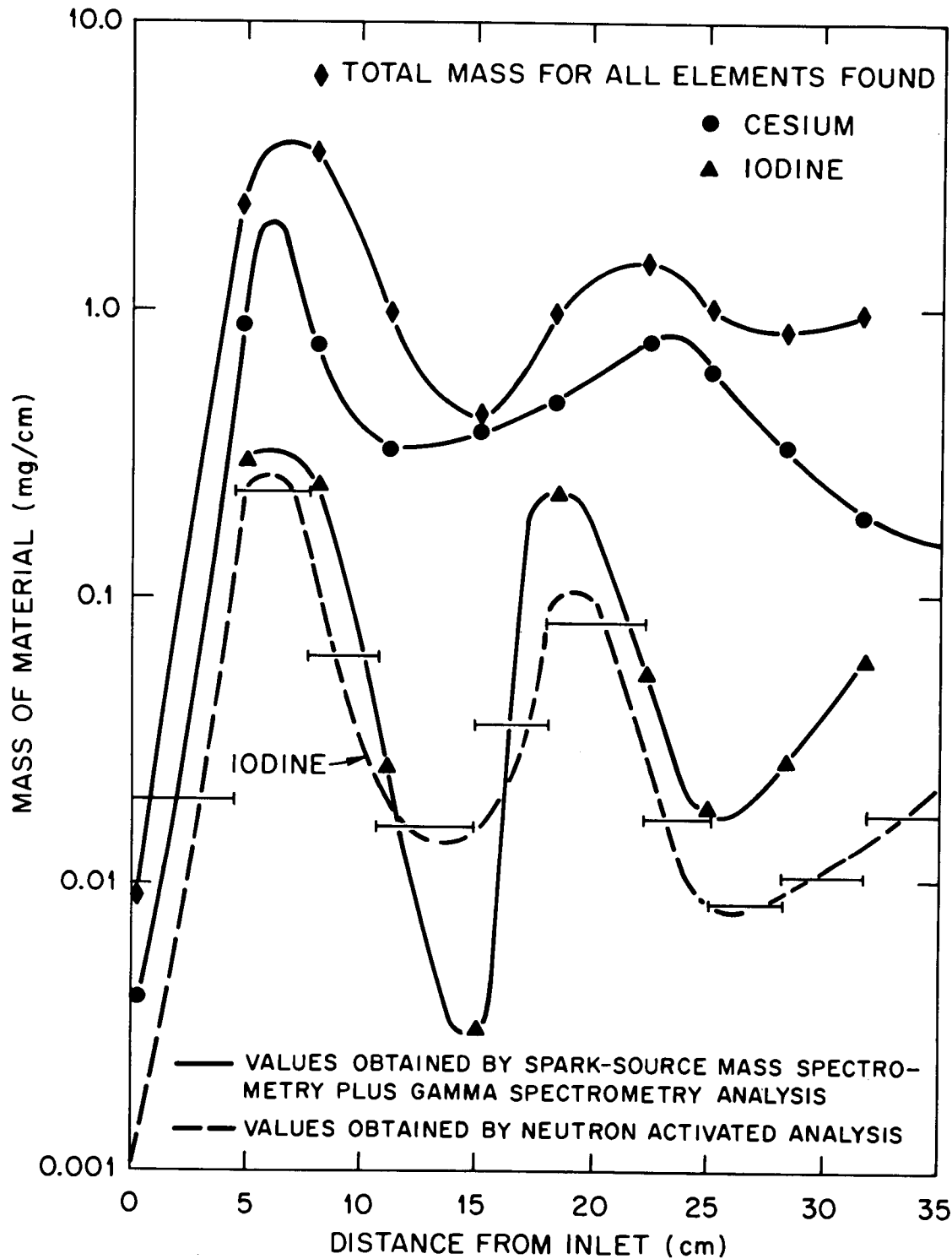


Fig. 13. Distribution of fission products cesium and iodine and total deposited material in the thermal gradient tube in test HI-4. (The temperature profile is given in Fig. 16.).

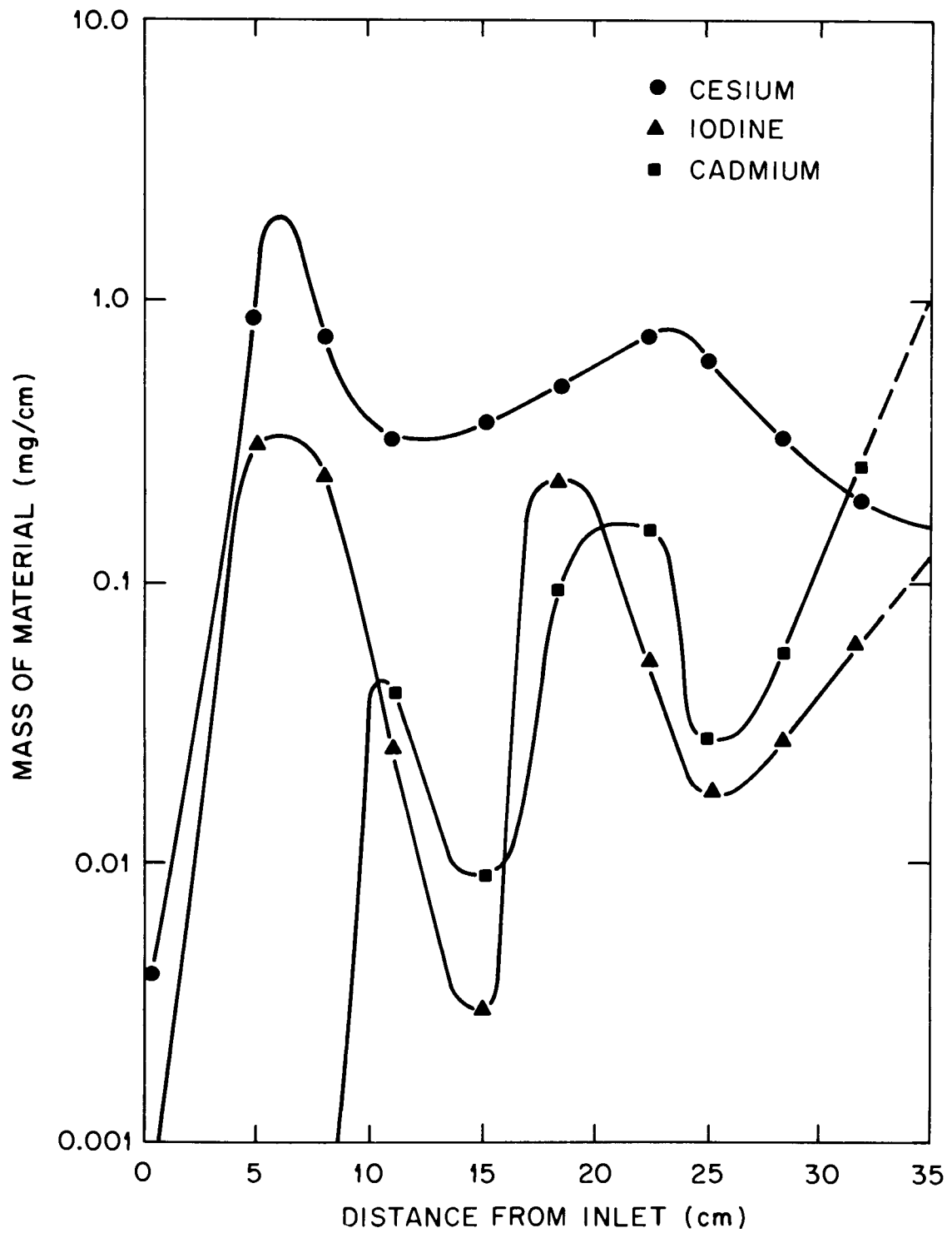


Fig. 14. Distribution of fission products cesium, iodine, and cadmium in the thermal gradient tube in test HI-4, as determined by SSMS analysis. (The temperature profile is given in Fig. 16.).

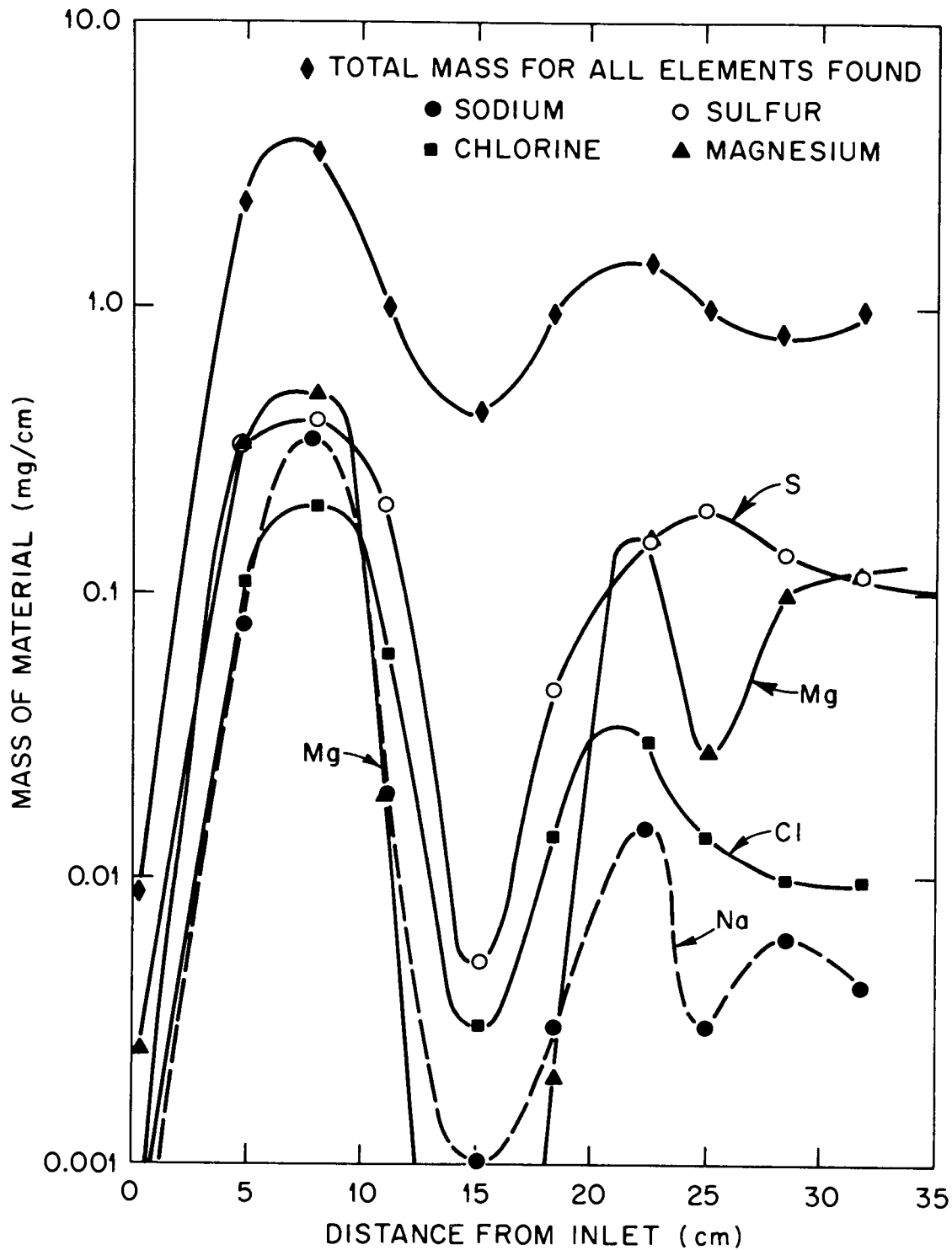


Fig. 15. Distribution of major contaminants along the thermal gradient tube after test HI-4, as determined by SSMS analysis. (The temperature profile is given in Fig. 16..)

The major contaminants in the aerosol deposit were Mg, S, Cl, and Na, which probably came from the zirconia ceramics used in the furnace. Figure 15 shows the deposition profiles of these materials along the thermal gradient tube.

Table 13 shows the fractions of test specimen inventories of certain fission products found in the thermal gradient tube and on the glass wool filter as determined by SSMS and gamma spectrometric analyses. Similar percentages of rubidium and cesium were found. This is reasonable because these elements are chemical analogs. The iodine fraction found (35%) was larger than the fraction found by neutron activation analysis (23%); however, as has already been pointed out, the value obtained by neutron activation analysis might be low. It is possible that some of the iodine might not have been removed by the leaching process. The amount of silver detected was similar to the amounts of cesium and rubidium detected. The indicated fraction of cadmium was ~80%. The analysis also showed trace amounts of Te, Ba, and Sr.

Table 13. Fission product release as determined by SSMS

Fission product	Fraction of test segment inventory found (%)
Cs	17
Rb	20
I	35
Ag	19
Cd	80
Te	<0.37
Ba	<0.015
Sr	<0.005

Includes only deposits in the thermal gradient tube and on the glass wool filter.

Cesium value determined by gamma spectrometry and used as a standard to determine others.

3.2.4 Thermal Gradient Tube Results

The thermal gradient tube in this experiment was a quartz tube (0.4 cm in internal diameter) lined with platinum foil to provide an inert deposition surface. When the furnace was at high temperature, the gas entering the thermal gradient tube was cooled; the heat was rejected radially by conduction in the gas and, subsequently, through the platinum liner, a small gas gap, and the quartz tube. The temperature gradient was measured by eight thermocouples attached outside the quartz. Four of these were used to control the four heaters that maintained the thermal gradient during the test. During the test, one of the heaters burned out. Figure 16 shows three temperature profiles that indicate how the

LOCATIONS AND NUMBERS OF PLATINUM TGT SECTIONS

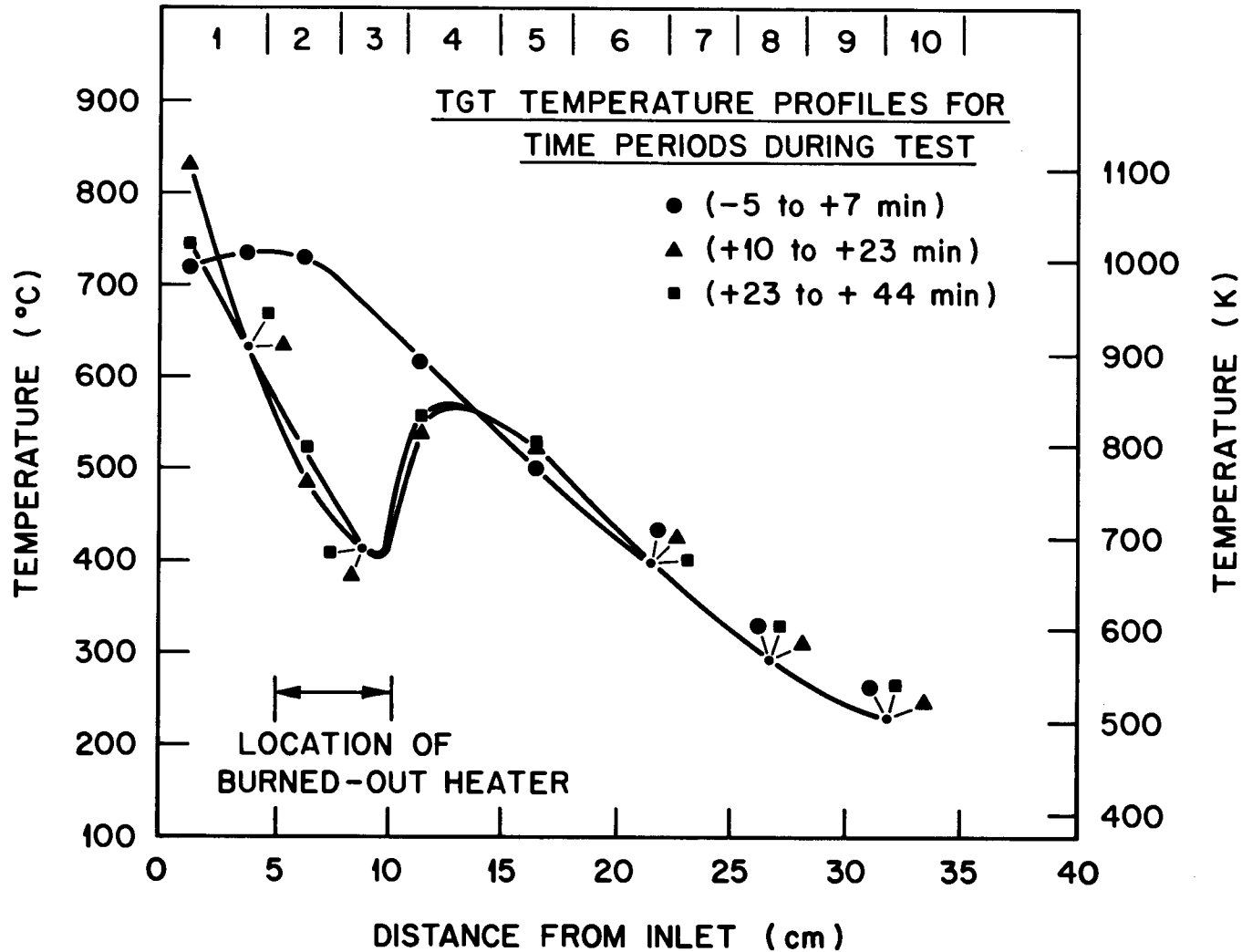


Fig. 16. Temperature distribution along thermal gradient tube in test HI-4.

temperature varied before, during, and after the 20-min period the fuel rod specimen was at 1850°C.

Appendix 1 of ref. 8 contains a simple calculation of the radial temperature distribution in the thermal gradient tube. Application of those methods to the conditions of test HI-4 gives the following relationship:

when the thermocouple temperature = XK ,
 then the inside surface of the platinum = $X + 5K$ and
 the center gas temperature = $X + 13K$.

Table 14 contains cesium and iodine data for the thermal gradient tube. The cesium profile is plotted against position in Fig. 17 and against temperature in Fig. 18. These data were obtained from the platinum thermal gradient tube liner after sectioning. The cesium profile was also measured by gamma scanning the intact platinum liner; the two measurements showed similar features but differed quantitatively. Figure 17 shows two peaks, at 6 and 23 cm, but we assume that the first peak is an artifact caused by the loss of temperature control and the resulting overcooling at that location. When the surface concentration of cesium is plotted against temperature, as shown in Fig. 18, the two peaks almost merge into one with a maximum ~ 750 K (477°C). Of the cesium that entered the thermal gradient tube, 47% deposited. The remainder (53%) was transported downstream where it was collected on the filters.

Figures 19 and 20 show the iodine deposition profile plotted against distance and temperature, respectively. It follows the cesium profile very closely, with the Cs/I mol ratio ranging from 6 to 10. Figure 19 shows a peak beginning at ~ 850 K (577°C) and reaching its maximum at ~ 780 K (307°C). There is also a small increase in iodine deposition 5 to 8 cm from the outlet end of the thermal gradient tube. Of the iodine that entered the thermal gradient tube, 37% deposited and 63% escaped and was trapped by the downstream filters.

Figure 21 shows that cesium was present on the thermal gradient tube in two forms that differed in their response to the basic leach; the subsequent acid leach, however, affected the residues equally. Below $\sim 350^\circ\text{C}$, the insoluble form constitutes about 0.2 to 0.4% of the cesium; above 350°C , it constitutes 4 to 34%.

Spark-source mass spectrometric data for test HI-4 (see Sect. 3.2.3) show that the less soluble cesium was found at the 11- to 18-cm location, where cesium is the principal material present. In test HI-2, radiogenic molybdenum was found to change in concentration with the insoluble cesium species; however, molybdenum was not detected in tests HI-3 and HI-4 by SSMS. No other correlation has been found between less soluble cesium and other elements.

Small amounts of ^{60}Co , ^{106}Ru , and ^{154}Eu were detected while the intact platinum liner of the thermal gradient tube was scanned by a Ge(Li) detector. The total quantities were:

Table 14. Fission products on thermal gradient tube in test HI-4

Section	Position (cm)	Temperature ^a		¹³⁷ Cs ^b (mCi)	Cs ^c (μg/cm ²)	¹²⁹ I ^d (μg)	I (μg/cm ²)
		(K)	(°C)				
1	0.0-4.6	850-1110	(577-837)	21	140	93	22
2	4.6-7.8	720-1010	(447-737)	170	1600	740	250
3	7.8-10.8	720-1010	(447-697)	56	580	190	66
4	10.8-14.9	770-910	(497-637)	49	370	65	17
5	14.9-18.1	740-820	(467-547)	45	440	120	39
6	18.1-22.2	660-760	(387-487)	86	640	290	76
7	22.2-25.2	590-660	(317-387)	83	850	53	19
8	25.2-28.2	540-590	(267-317)	46	470	25	9
9	28.2-31.6	500-540	(227-267)	35	310	37	12
10	31.6-34.9	470?-500	(197-227)	17	160	57	18

^aTemperature of platinum deposition surface. Temperature ranges overlap because heater No. 2 burned out.

^bCounted after sectioning; allowance made for attenuation of 662-keV gamma ray of ¹³⁷Cs by air and glass vial. Decay corrected to July 15, 1981.

^cORIGEN calculation gives specific activity of cesium as 34.4 Ci ¹³⁷Cs/(g·total cesium) on July 15, 1981.

^dORIGEN calculation gives ¹²⁹I as 75.8% of total iodine on July 15, 1981.

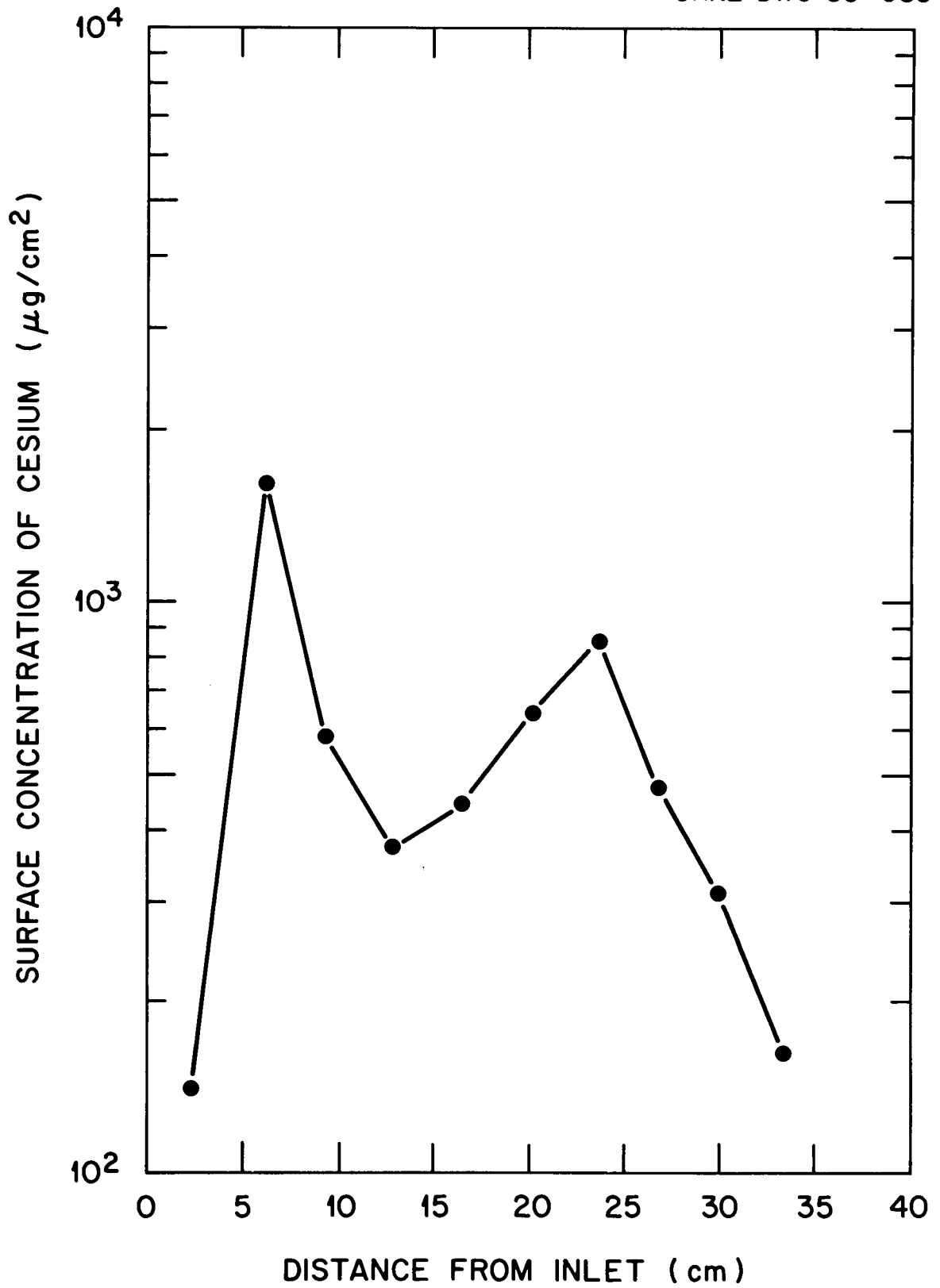


Fig. 17. Cesium profile along thermal gradient tube in test HI-4.

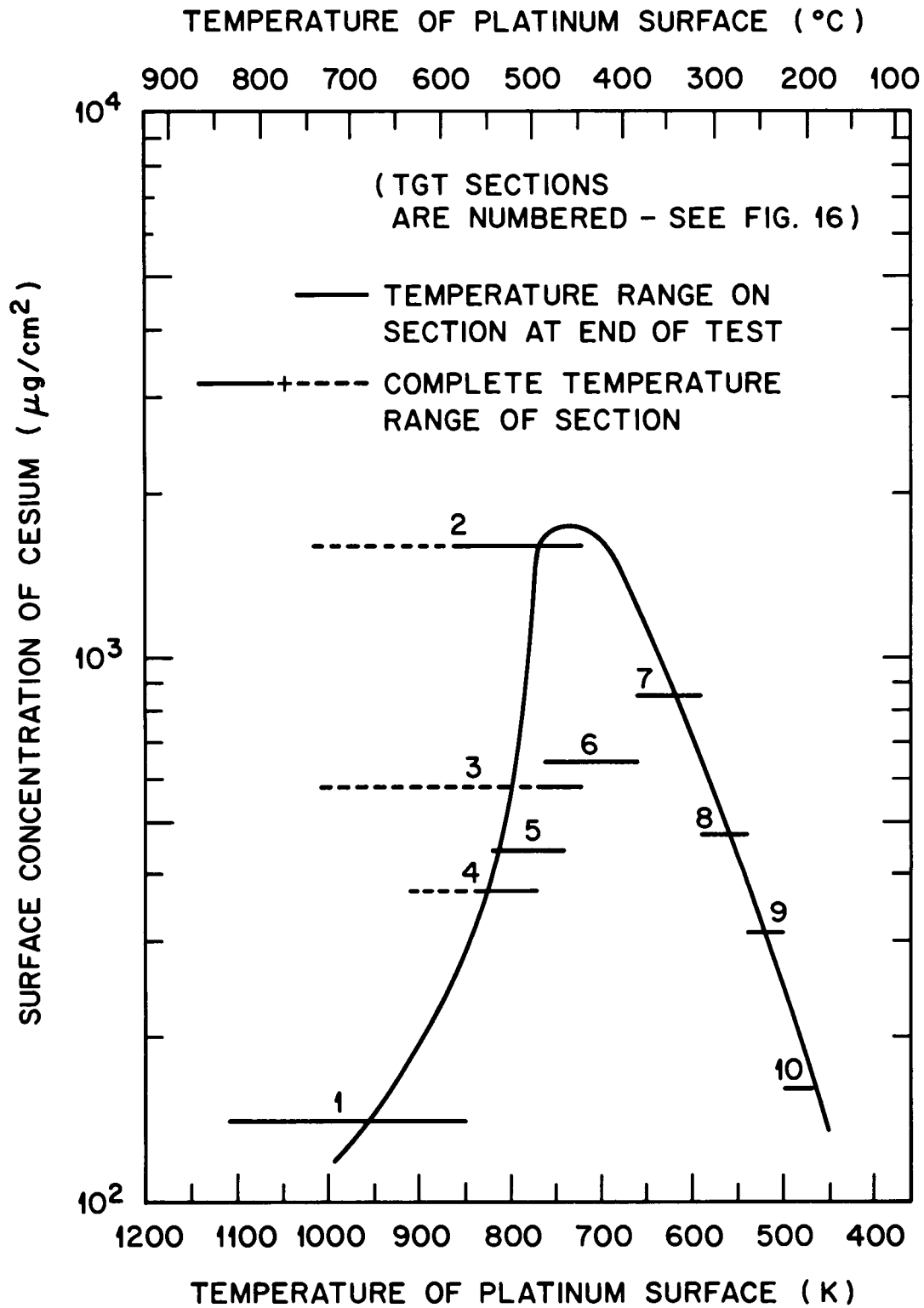


Fig. 18. Cesium profile along thermal gradient tube in test HI-4 as a function of the temperature of the deposition surface.

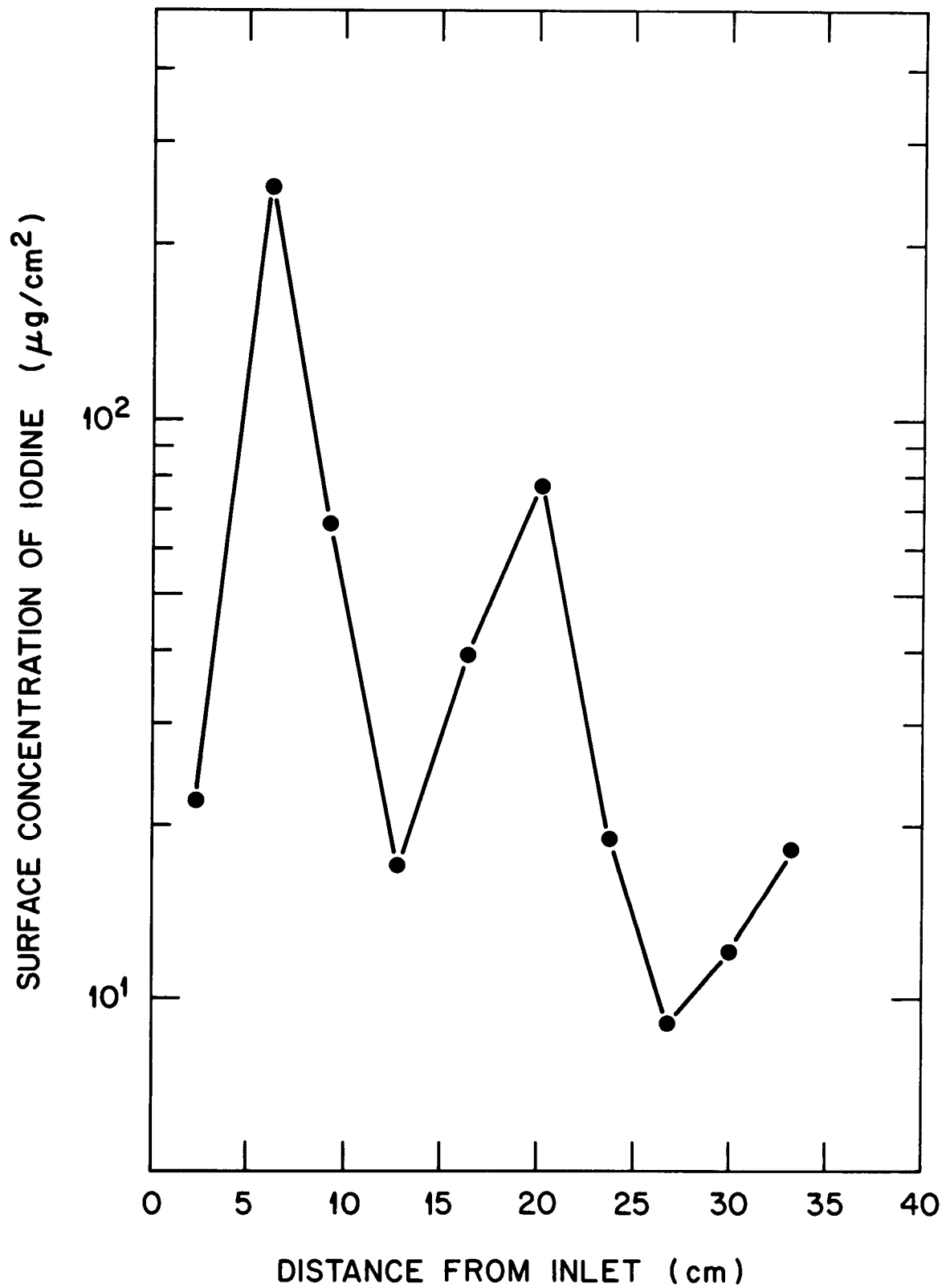


Fig. 19. Iodine profile along thermal gradient tube in test HI-4.

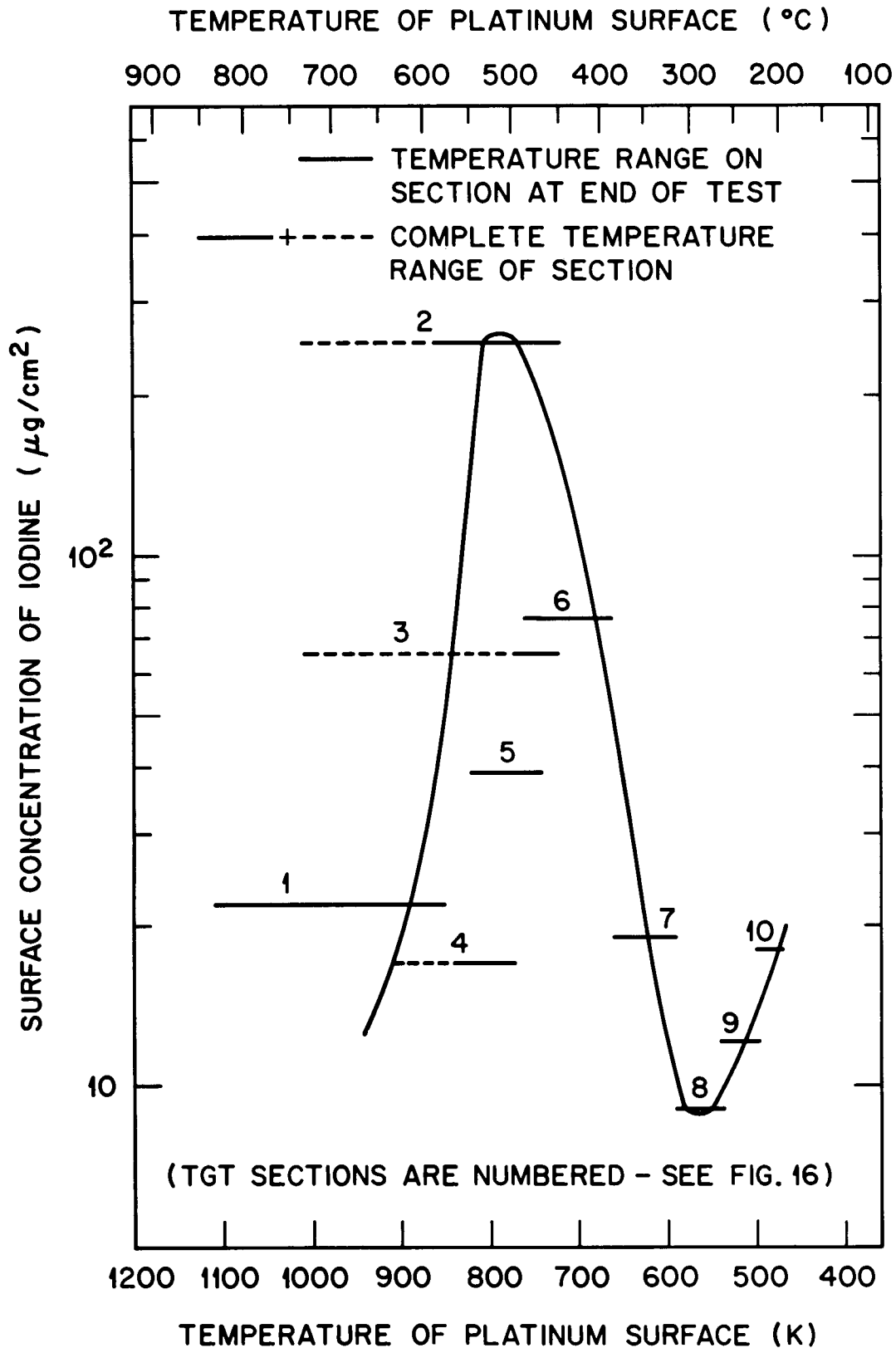


Fig. 20. Iodine profile along thermal gradient tube in test HI-4 as a function of the temperature of the deposition surface.

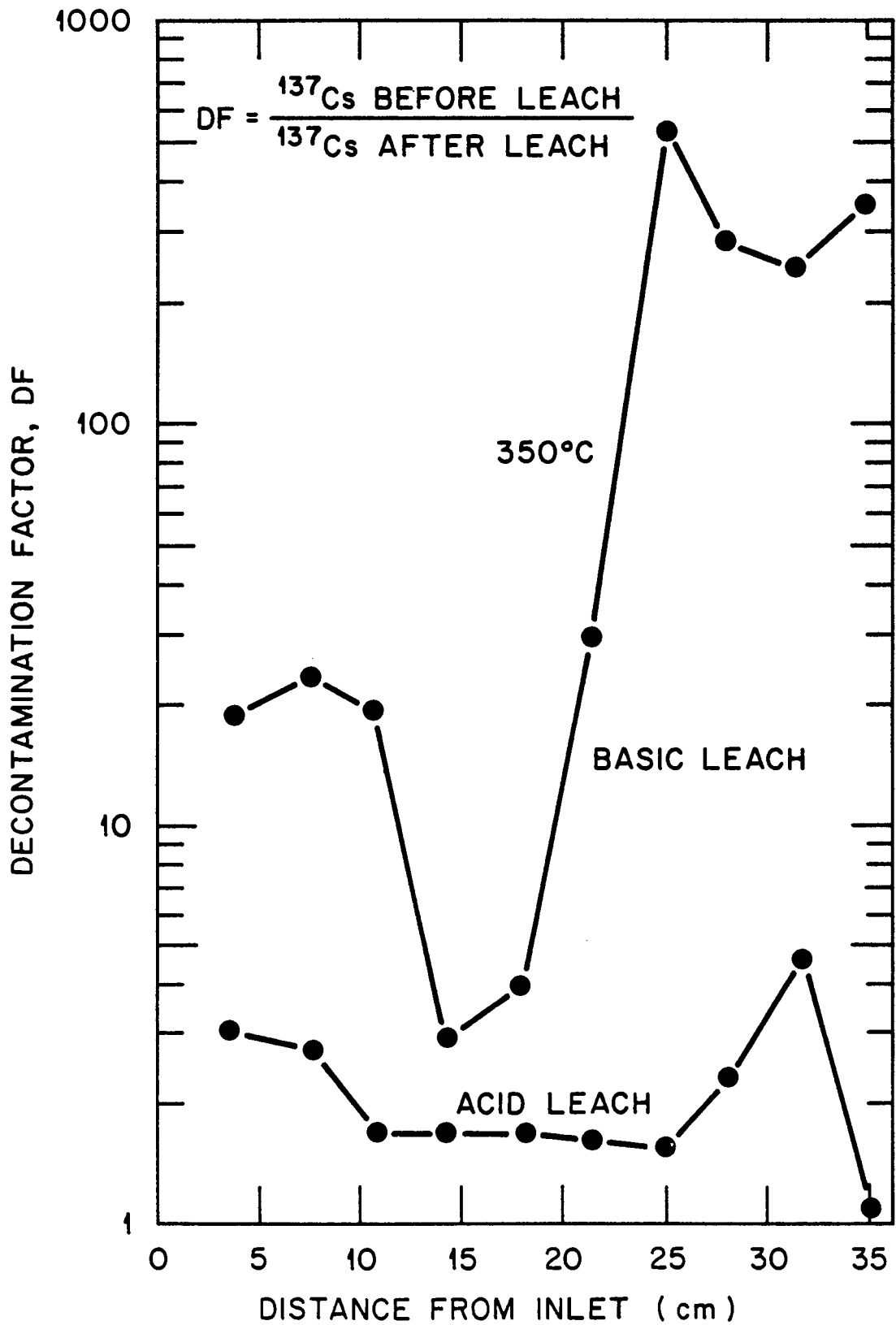


Fig. 21. Solubility of cesium deposited in the thermal gradient tube of test HI-4: comparison of basic and acidic leaches.

- 41 μCi ^{60}Co (0.15% of inventory) ,
 163 μCi ^{106}Ru (0.01% of inventory) ,
 119 μCi ^{154}Eu (0.04% of inventory) .

These numbers contain an unknown contribution from the gamma background in the counting area (perhaps 4 μCi for ^{60}Co , and less for Ru and Eu) and, thus, are imprecise. Also, the high levels of ^{134}Cs and ^{137}Cs on much of the platinum mask the small peaks from Co, Ru, and Eu.

Cobalt-60 was detected at levels between 4 and 8 $\mu\text{Ci}/\text{cm}$ between 10 and 15 cm from the gas inlet. Downstream, it occasionally appeared at levels of 1 to 2 $\mu\text{Ci}/\text{cm}$. No cobalt was found by SSMS analysis.

Ruthenium-106 was detected at 37 to 47 $\mu\text{Ci}/\text{cm}$ on the last 4 cm at the outlet end. No ruthenium was found by SSMS analysis.

Europium-154 decreased from 22 $\mu\text{Ci}/\text{cm}$ at 10 cm to 7 $\mu\text{Ci}/\text{cm}$ at 15 cm and thereafter appeared twice at ~ 5 $\mu\text{Ci}/\text{cm}$. Very low levels were detected by SSMS on surfaces at the outlet end but not elsewhere. It is difficult to explain this disagreement; it is possible that the SSMS sampling technique may not have removed the europium from the platinum if it were fixed in place on the higher-temperature sections of the thermal gradient tube.

3.2.4.1 Interpretation: cesium and iodine on the thermal gradient tube

Both the cesium and iodine profiles peaked and then subsided toward the outlet end of the thermal gradient tube; the downstream side of the peak was steeper in test HI-4 than in tests HI-1 and -2. Quantitatively, the results were:

<u>Experiment</u>	<u>Gas flow (L/min at 423 K)</u>	<u>Iodine profile gradient (decades/cm)</u>
HI-1	2.1	0.05
HI-2	1.9	0.04
HI-3	1.0	0.20
HI-4	1.1	0.14

High gas flow rates seem to cause broad profiles, as was noted in ref. 15.

During test HI-4, 0.643 mol of gas passed down the thermal gradient tube during the 20 min that the fuel specimen was at maximum temperature, carrying 35 μmol iodine atoms and 270 μmol cesium atoms. If these were present as CsI and CsOH, the time-averaged partial pressures at the entrance to the thermal gradient tube were:

CsI: 5.4×10^{-5} bar ,

CsOH: 3.6×10^{-4} bar .

Time-averaging is justified for cesium (and also for krypton) because on-line gamma spectrometry of the whole thermal gradient tube showed that ^{137}Cs built up at a constant rate. In the absence of time-rate data for iodine, we assume similar behavior.

The saturated vapor pressure of CsI (in bar) over pure CsI depends on temperature (in K):

$$\log_{10}P = 6.243 - 9699/T,^{17} \quad (1)$$

$$\log_{10}P = 17.47 - 3.52 \log_{10}T - 9678/T \text{ (more recent data).}^{18} \quad (2)$$

Deposition of pure CsI is expected to begin under the conditions of test HI-4 when the thermal gradient tube thermocouples read 852 to 928 K (579 to 655°C). (The range reflects the different equations for CsI partial pressure in the literature.) Figure 20 shows this to be the case, although the data are confusing because temperature control was lost on the thermal gradient tube. There is no need to propose a solid solution of CsI in another cesium compound as the solid phase, as was proposed for test HI-3.¹⁵

In summary, iodine behavior was consistent with its release as CsI, part of which condensed on the platinum and the remainder collected as an aerosol on the filters downstream.

The primary cesium compound has not yet been identified. Pure CsOH, which is more volatile than CsI, will begin to deposit when the thermocouples on the thermal gradient tube read 755 K¹⁹ (482°C) or 797 K²⁰ (524°C). In the test the major cesium compound on the thermal gradient tube was less volatile than CsOH; it may have contained sulfur (from the furnace ceramics). The SSMS data showed considerable amounts of sulfur on the thermal gradient tube, which suggests that Cs_2S , Cs_2SO_3 , or Cs_2SO_4 may have been present.

3.2.5 Aerosol Characteristics

In severe accident analyses, increasing attention is being paid to the transport of fission products as aerosols. Aerosol particles formed during accidents are expected to be mixtures of materials vaporized from the UO_2 fuel (mainly fission products), Zircaloy cladding, Inconel grid spacers, stainless steel control rod cladding, and Ag-In-Cd or B_4C control materials. In these tests the only aerosol sources have been the fuel and cladding, along with spurious material released from ceramics in the high-temperature furnace design. Tests with spacer and control materials to provide the complete accident atmosphere are planned for the future.

We have begun the development of methods for characterization of aerosols formed in our tests using SSMS, weighing, scanning electron microscopy (SEM), and energy-dispersive x-ray analyses of representative particles. The characterization of aerosols is complicated by the gradual change in composition as vapors condense to form solid particles or condense, sorb, or react with previously formed particles. In the furnace,

all of the released material is vapor except for any mechanically produced particles. Even at the entrance to the thermal gradient tube (900°C), most of the released material remains a vapor. Based on the shape of the deposition profiles, most of the material in the thermal gradient tube was deposited on the liner surfaces via condensation. Materials leaving the thermal gradient tube are believed to be almost entirely solid aerosol particles. The composition of the condensed vapors (the deposits in the thermal gradient tube) and the aerosol solids (the material collected on the glass wool and high-efficiency filters) has been measured in every HI-series test and is discussed in Sect. 3.2.3 for test HI-4.

The masses of vapor and aerosol deposits in tests HI-1 and HI-2 were measured by summing the quantities of the various elements as determined by SSMS. Both pretest and posttest weights of these deposits were measured directly in tests HI-3 and -4. Figure 22 shows the typical grayish-black appearance of the deposit on the prefilter which was used in test HI-4. Table 15 provides values of the mass collected and estimated aerosol concentration for each of the tests. In test HI-4, the values for the thermal gradient tube and prefilter were obtained both by SSMS analysis and by weighing; note the good agreement.

3.2.6 Metallographic Examination of Fuel Specimen

As was discussed in Sect. 2.5, the fuel specimen, zirconia boat, and zirconia furnace tube liner were encased in epoxy resin and cut into 2.54-cm-long pieces for inspection. The transverse cross sections are illustrated in Fig. 23. There is evidence of cladding melting in each of the sections, which indicates that every portion of the specimen was at a temperature $>1760^{\circ}\text{C}$ during the test.¹⁶ Furthermore, there was an apparent gradient in the degree of melting, with the most extensive melting occurring at the inlet end. This implies that there was a temperature gradient along the fuel rod specimen during the test. A temperature of $\sim 1850^{\circ}\text{C}$ was reached and maintained at the inlet end of the fuel specimen, as determined by a calibrated optical pyrometer. Results of a posttest temperature calibration test suggested that an axial gradient of $\sim 100^{\circ}\text{C}$ may have been present, but the evidence of cladding melting indicates that the gradient was $<100^{\circ}\text{C}$.

Three of the transverse sections shown in Fig. 23 were selected and prepared for metallographic examination. These sections, numbered 0, 3, and 7 (which were, respectively, 0.3, 7.6, and 17.8 cm from the inlet end of the fuel specimen), are shown in Fig. 24. They illustrate the appearance of the test specimen at the inlet end (section 0, where maximum temperature and oxidation occurred), near the mid-length (section 3), and near the outlet end (section 7, where the temperature was slightly lower and oxidation was less extensive because of steam depletion). The particular areas photographed at high magnification are indicated by the numbers 1, 2, and 3 on the sections in Fig. 24.

These views show the pool of formerly molten cladding that ran down and contacted the ZrO_2 boat which supported the test specimen. This pool of melt was largest in section 0. Voids that formed in the molten cladding

PHOTO Y190169

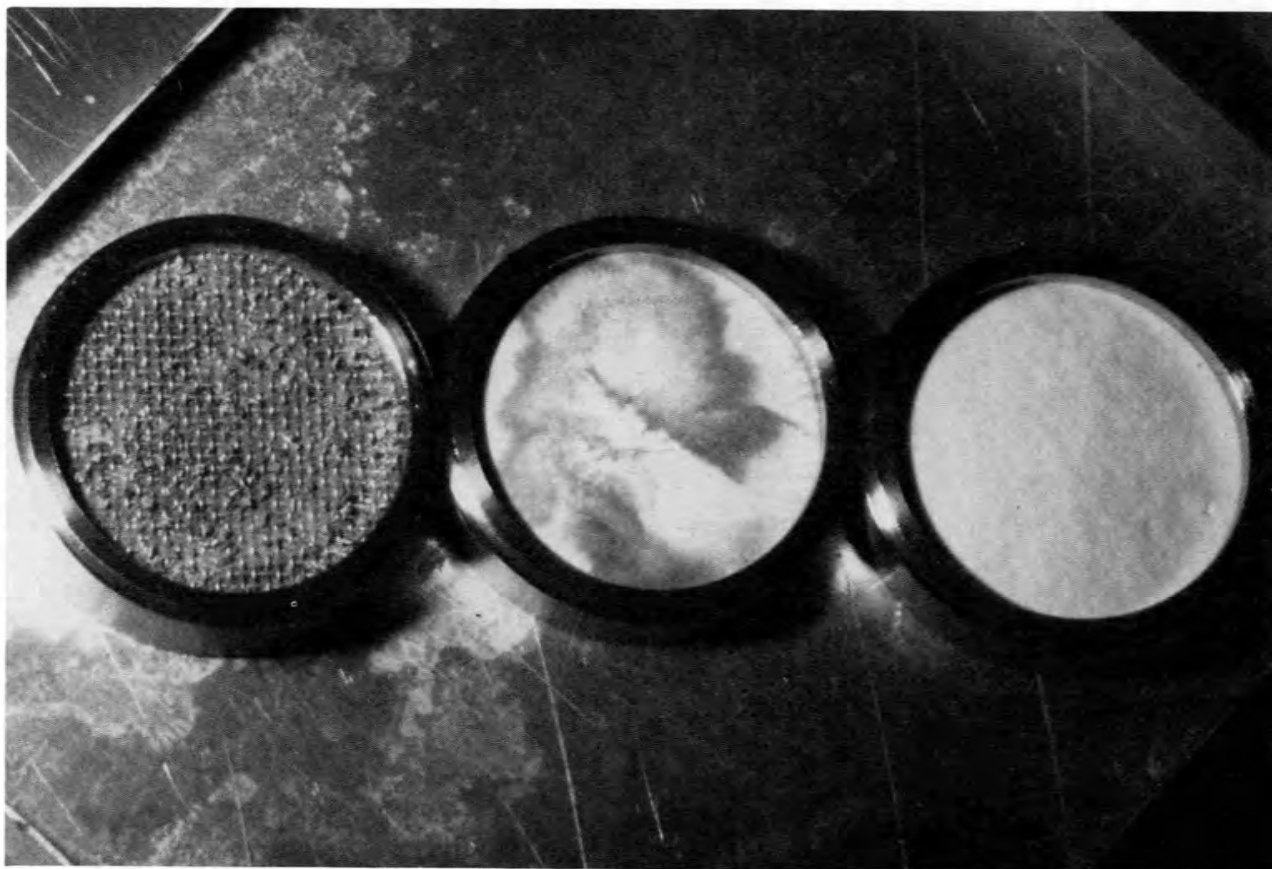


Fig. 22. Appearance of filters from test HI-4; from the left, screen covering glass wool prefilter, first HEPA, and second HEPA.

Table 15. Aerosol particles and vapor produced in fission product release tests

Test No.	Temperature (°C)	Mass collected on thermal gradient tube (mg)	Mass collected on filter (mg)	Aerosol concentration ^a (g/m ³)	
				At furnace ^b temperature	At 100°C ^c
HI-1 ^d	1400	~5	~18	<0.1	~0.4
HI-2 ^e	1700	70 ± 5	230 ± 5	1.6	7.0
HI-3 ^e	2000	80 ± 5	220 ± 5	2.5	15.0
HI-4 ^e	1800 ^f	30 ± 5 (~40) ^d	70 ± 5 (~75) ^d	0.73	4.3

^a Assumes test time plus 5 min for aerosol production time.

^b Essentially all of the released material would be vapors at the furnace temperature.

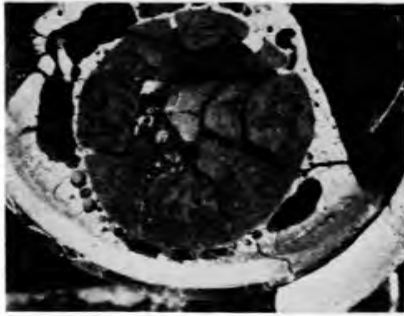
^c Essentially all of the released material would be solids at 100°C.

^d Mass of deposits estimated from mass spectrometric data.

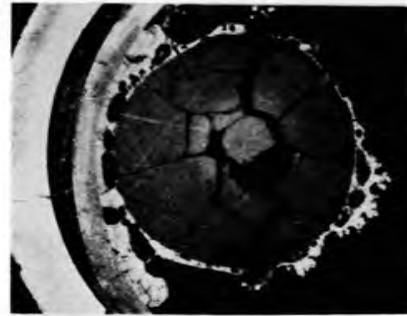
^e Mass of deposits determined by weighing thermal gradient tube and filters.

^f Temperature at the inlet Zircaloy end cap of the test specimens was ~1850°C; temperature at the outlet Zircaloy end cap was >1760°C.

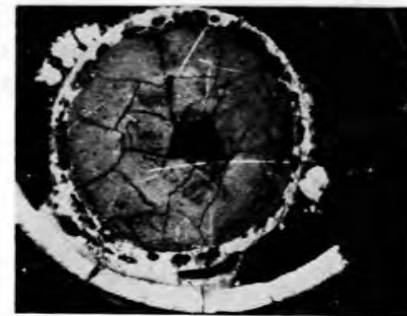
PHOTO-R78223



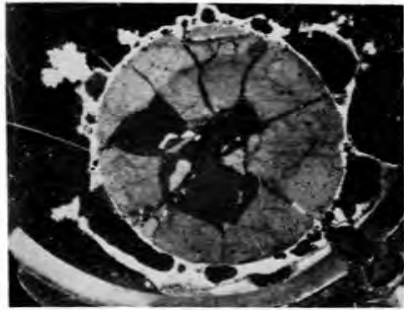
0



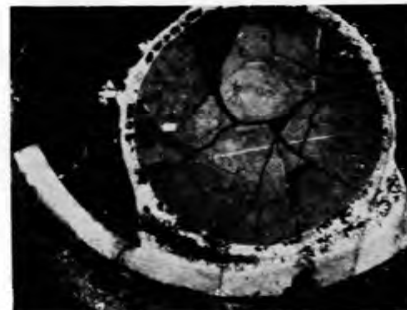
1



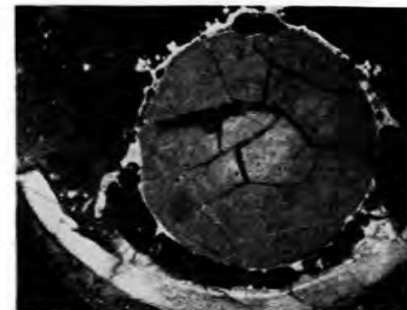
2



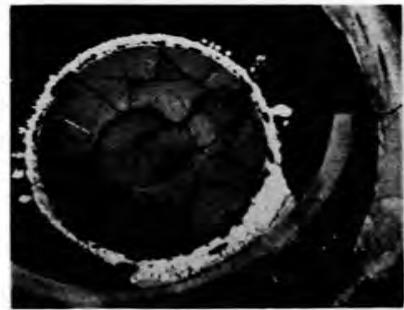
3



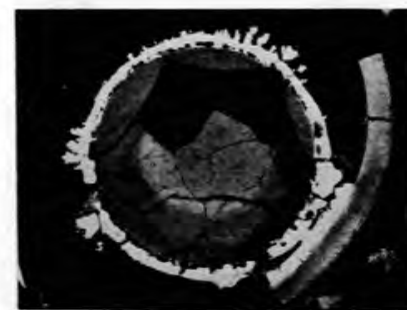
4



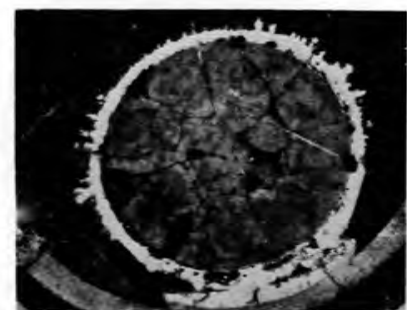
5



6



7



8

Fig. 23. Sections of fuel specimen and ZrO_2 ceramics from test HI-4; sections were cut at 1-in. intervals, with cut 1 at the inlet end.

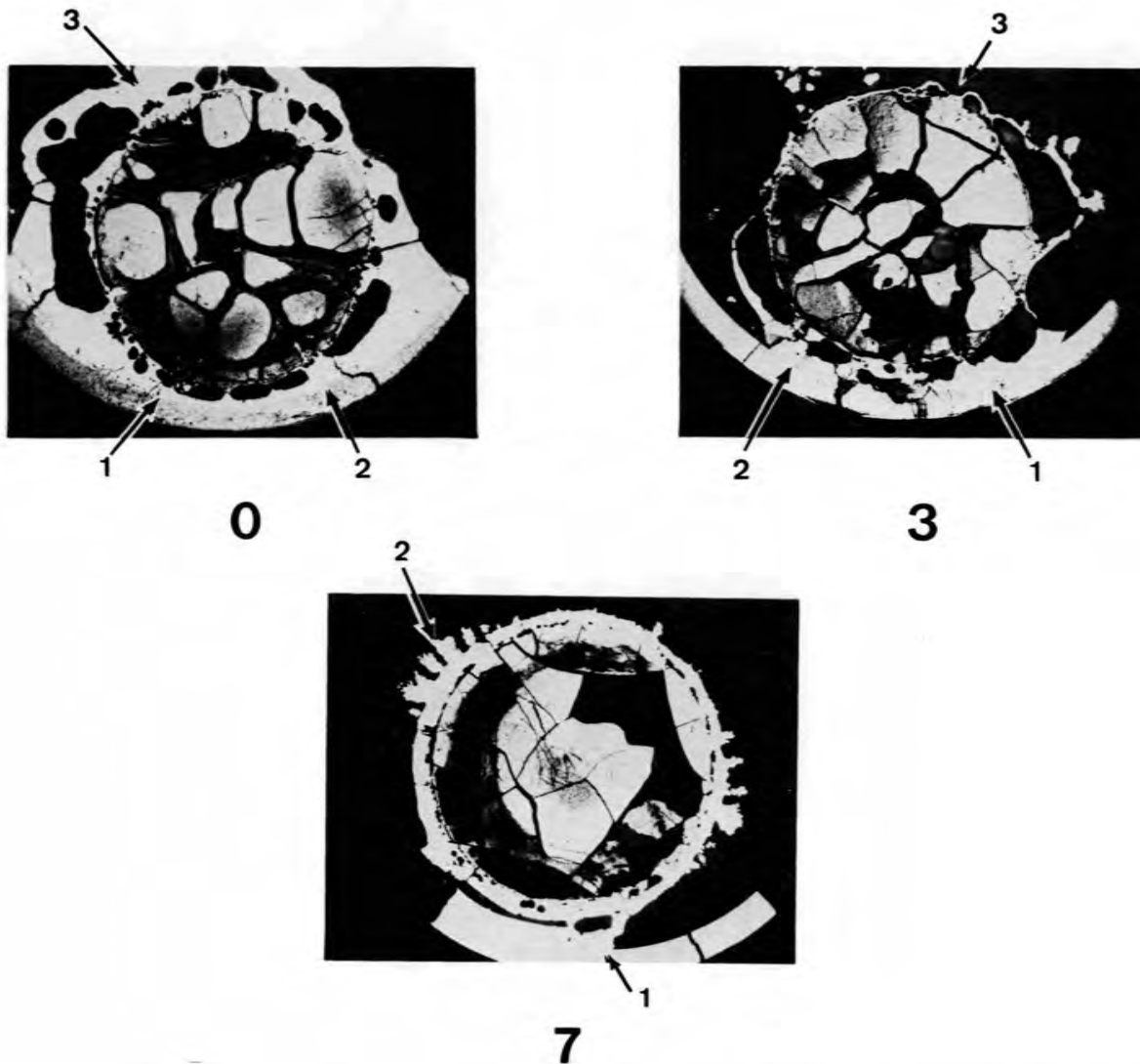


Fig. 24. Transverse sections from test HI-4 that were examined metallographically. The numbers 1, 2, and 3 identify areas photographed, some of which are shown in Fig. 25.

were much larger in sections 0 and 3 than in section 7; the size and extent of the large voids suggest that gas released from the fuel while the cladding was molten may have been the mechanism of formation. Penetration and destruction of the ZrO_2 boat by the molten Zircaloy are apparent in the first two sections. Wetting of both the UO_2 fuel and the ZrO_2 boat by the Zircaloy, although extensive in sections 0 and 3, was limited in section 7. An unusual structure, a series of projections growing outward from the cladding (area 2 in section 7), was observed and selected for detailed examination.

Areas 1 and 2 in both sections 0 and 3 showed similar structures. The molten Zircaloy had oxidized sufficiently to wet both the ZrO_2 boat below and the UO_2 fuel above the pool. The gray metallic phase in Fig. 25 and in the higher-magnification view in Fig. 26 is α -Zr(O), which can contain up to ~6% oxygen by weight. Both this phase and the bright metallic phase (probably mostly zirconium) may contain uranium as a result of UO_2 reduction by zirconium, but this needs to be confirmed. As would be expected, the molten metallic phases penetrated cracks in the UO_2 (Fig. 25) in a number of areas.

Area 3 of section 3 (Fig. 27) illustrates the appearance of the cladding along the top of the test specimen over most of its length. Two large and many small voids, along with extensive oxidation, are apparent in the previously molten cladding. Significant amounts of gas, perhaps fission product vapors from the fuel, must have been present to form these large voids. Except for the interfaces with the molten cladding, no significant changes in the UO_2 were seen. A higher-magnification view of the oxidized cladding, shown in Fig. 28, revealed at least three phases: ZrO_2 , α -Zr(O) [or α -U, Zr(O)], and an alloy, probably U, Zr.

In area 2 of section 7, near the outlet end of the test specimen, several of the unusual projections which grew at right angles from the cladding were examined (Fig. 29). These projections apparently contain some ZrO_2 , along with larger fractions of two unidentified metallic phases. Further examination and positive identification of all phases will be attempted and reported later.

3.2.7. Determination of Cesium Release by Gamma-ray Spectrometric Analysis of the Fuel Rod Segment Before and After Test HI-4

A relatively simple method of determining the percentage of cesium which was released during test HI-4 was devised. Gamma spectrometry values for the isotopes ^{134}Cs (1365 keV) and ^{154}Eu (1275 keV) in the fuel rod segment before and after the test were measured and compared. Europium-154 was chosen because it was not released during the test, and because it had a high energy peak similar to that of ^{134}Cs . Thermodynamic calculations suggest that europium is probably present in LWR fuel as Eu_2O_3 .²¹ If so, because of its low volatility, little migration of europium would have occurred in the segment during the test.

One important criterion needed for the method of determining release is that the physical state of the fuel not be altered much by the test

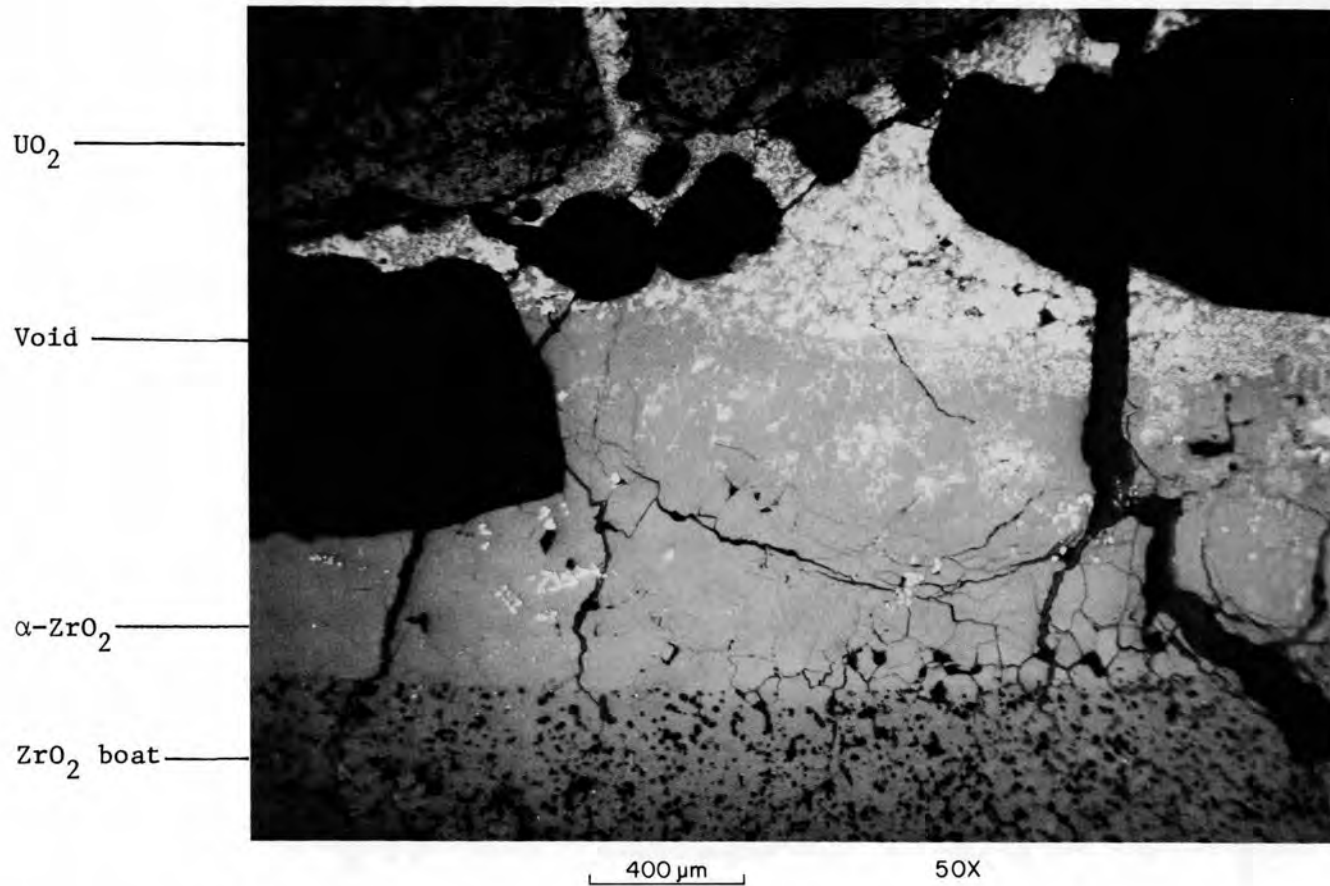


Fig. 25. View of area 2, section 0 in Fig. 24, showing interaction zones at molten cladding/ UO_2 interface (above) and molten cladding ZrO_2 boat interface (below).

PHOTO-R78559

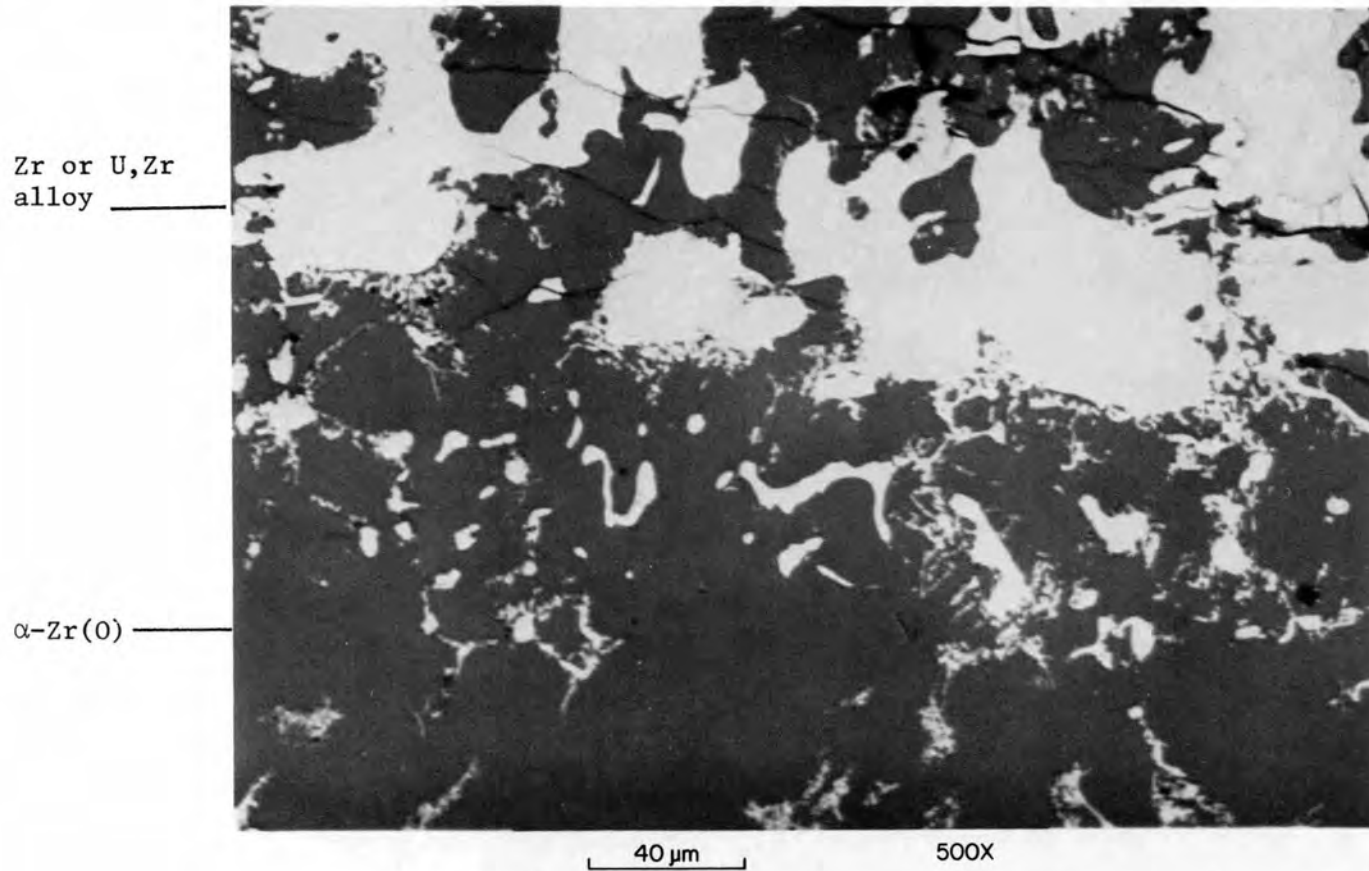
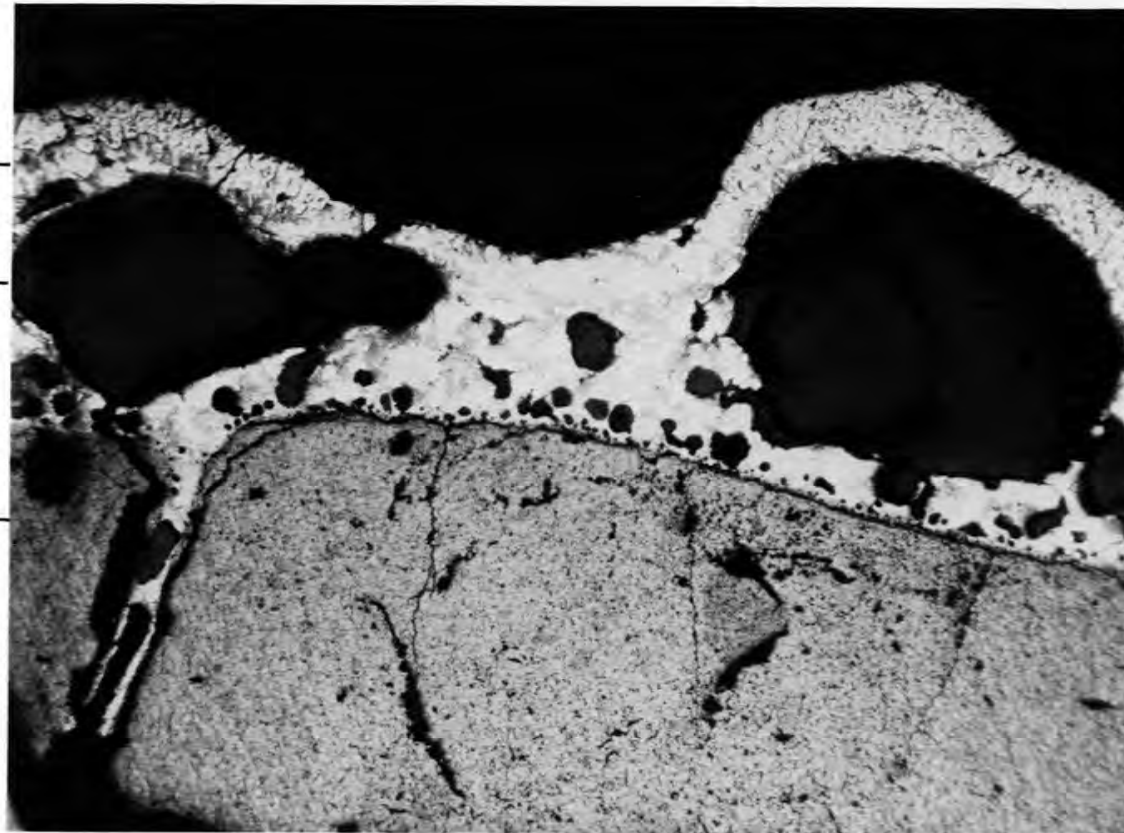


Fig. 26. Higher-magnification view of area from upper region in Fig. 24, showing two metallic phases.

Oxidized
cladding
($ZrO_2 + ?$)

Void

UO_2



400 μ m

50X

Fig. 27. View of a small region from area 3 of section 3 (see Fig. 24) showing large voids in the previously molten cladding and penetration of the melt into a crack in the UO_2 . The cladding contains ZrO_2 plus other unidentified phases.

PHOTO-R78574

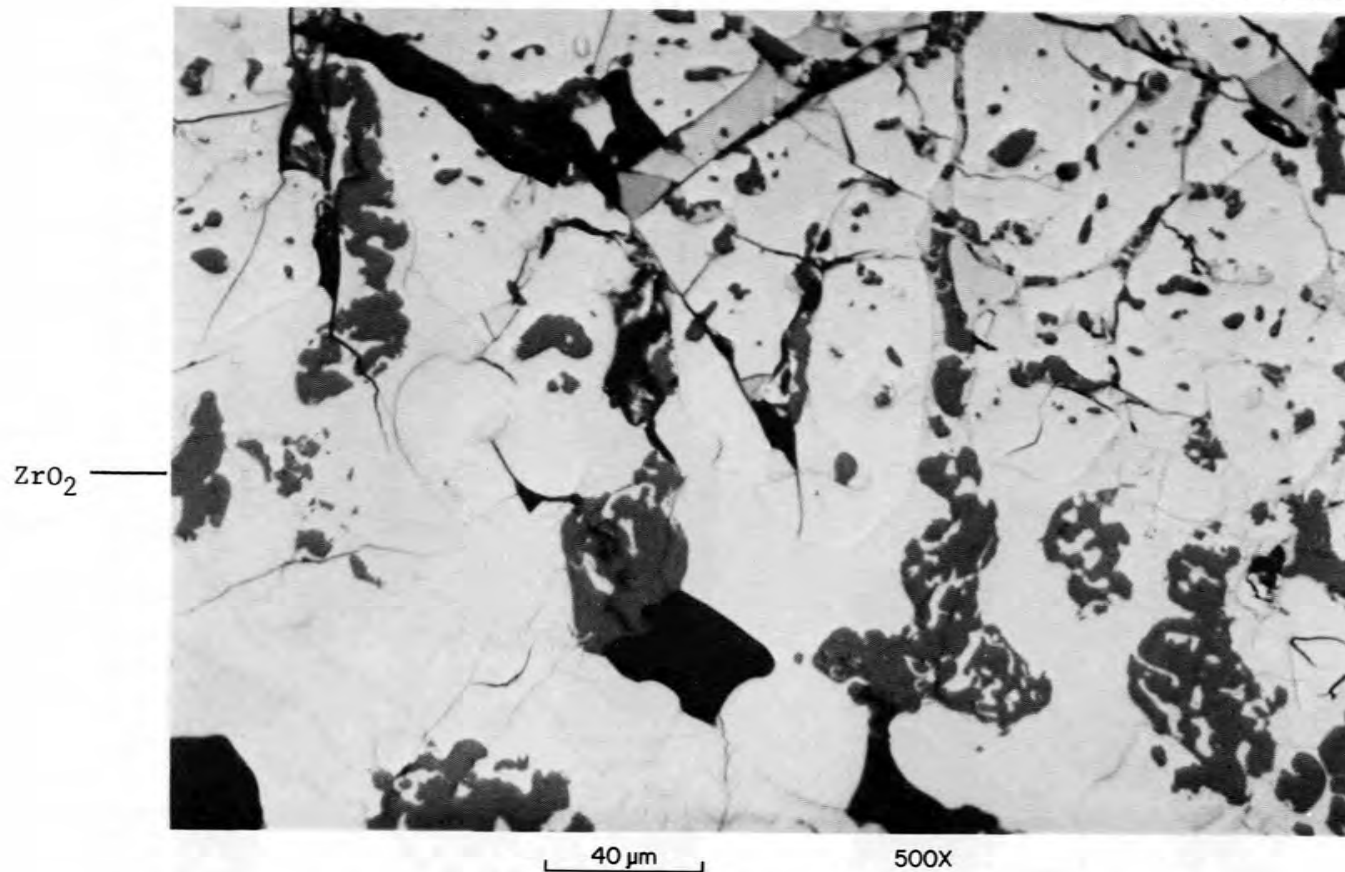


Fig. 28. Higher-magnification view of melted cladding region above the large void on the left in Fig. 27. Gray phase is ZrO_2 ; metallic phases probably are (U,Zr) alloy and $\alpha-U,Zr(O)$.

400 μm

50X

Fig. 29. View of area 2, section 7 (see Fig. 24), showing projections from cladding which were observed in several regions of this section. These projections contain a small fraction of ZrO_2 plus two other unidentified phases.

conditions or by posttest handling. These conditions were observed in test HI-4.

Since the gamma-ray energies were relatively high and almost the same, an attenuation correction factor for ^{134}Cs (1365 keV) was determined by dividing the pretest activity of ^{154}Eu (1275 keV) by the posttest value.

The following calculations show how the percentage of ^{134}Cs release was obtained:

- Attenuation correction factor (for epoxy, ZrO_2 liner, etc.),

$$F = \frac{\text{Pretest } ^{154}\text{Eu (1275-keV) value}}{\text{Posttest } ^{154}\text{Eu (1275-keV) value}} = \frac{1.460 \times 10^5 \mu\text{Ci}}{1.275 \times 10^5 \mu\text{Ci}} = 1.1457 ;$$

- % ^{134}Cs released = % cesium released,

$$\% = \frac{[\text{Posttest } ^{134}\text{Cs (1365-keV) value}] F}{\text{Pretest } ^{134}\text{Cs (1365-keV) value}} \times 100 ,$$

$$\% = \frac{(5.040 \times 10^5 \mu\text{Ci})(1.1457)}{(8.988 \times 10^5 \mu\text{Ci})} \times 100 = 35.8 .$$

This value compares very well with the value of 31.7%, which was obtained by counting the individual apparatus components (see Table 10).

4. CONCLUSIONS

This report presents only a limited evaluation and interpretation of the data obtained in test HI-4. Further evaluation, interpretation, and correlation will be included in a topical report, which will consider the results of several tests over a range of experimental conditions. The following observations and conclusions should be considered of a preliminary nature:

1. This was the first test in the current experimental series to be conducted with BWR fuel. The test specimen was heated at $1800 \pm 50^\circ\text{C}$ for 20 min in an atmosphere of flowing steam (0.32 L/min) and helium (0.30 L/min). Based on the measured amount of hydrogen generated, ~54% of the Zircaloy cladding was oxidized.
2. Continuous gamma-ray spectrometric monitoring of ^{137}Cs and ^{85}Kr during the test revealed, as was the case in previous tests, that the rate of release of these fission products increased immediately after the power was turned off and the fuel specimen began to cool.
3. Based on gamma-ray spectrometric and neutron activation analyses, 31.7% of the ^{137}Cs , 21.1% of the ^{85}Kr , and 24.7% of the ^{129}I contained in the specimen were released. If the pellet-clad gap inventory of fission gas inventory had also been available for release, the ^{85}Kr release would have been 31.3%.

4. A cesium release value of 35.8% was obtained by gamma-ray spectrometric analysis of the fuel rod segment before and after the test.
5. Only trace amounts of ^{125}Sb were detected. This behavior is expected when the Zircaloy cladding is not totally oxidized or removed from the pellets, and very high levels of ^{134}Cs and ^{137}Cs are present.
6. The results of SSMS analyses were in very good agreement with results obtained by gamma spectrometry and neutron activation. The fission products detected, other than Cs and I, were Rb, Br, Ag, and Cd. The release and deposition behavior of Rb and Br was similar to that of their chemical analogs Cs and I. Cadmium and silver appeared to be more volatile, as was evident by their collection at the cooler end of the collection system.
7. The masses of deposits in the thermal gradient tube and on the glass wool prefilter, as determined by SSMS and gamma spectrometric data, were about 40 and 75 mg, respectively. These values were in good agreement with actual values obtained by weighing the components before and after the test, 35 ± 5 and 70 ± 5 mg.
8. The presence of many large voids suggests that rapid gas release (the fission product gases Kr and Xe and perhaps vapors of I, Cs, and Te) from the UO_2 occurred while the cladding was molten. Although not confirmed, the presence of uranium, as $(\text{U,Zr})\text{O}_2$, $\alpha\text{-U,Zr(O)}$, and/or U,Zr alloy in the oxidized cladding appears likely.

5. REFERENCES

1. M. F. Osborne, R. A. Lorenz, and R. P. Wichner, "Program Plan for Fission Product Release from LWR Fuel in Steam," memorandum to USNRC, April 1982.
2. R. A. Lorenz, J. L. Collins, A. P. Malinauskas, O. L. Kirkland, and R. L. Towns, Fission Product Release from Highly Irradiated LWR Fuel, NUREG/CR-0722 (ORNL/NUREG/TM-287/R2), February 1980.
3. R. A. Lorenz, J. L. Collins, A. P. Malinauskas, M. F. Osborne, and R. L. Towns, Fission Product Release from Highly Irradiated LWR Fuel Heated to 1300-1600°C in Steam, NUREG/CR-1386 (ORNL/NUREG/TM-346), November 1980.
4. R. A. Lorenz, J. L. Collins, M. F. Osborne, R. L. Towns, and A. P. Malinauskas, Fission Product Release from BWR Fuel Under LOCA Conditions, NUREG/CR-1773 (ORNL/NUREG/TM-388), July 1981.
5. R. A. Lorenz, J. L. Collins, and A. P. Malinauskas, Fission Product Source Terms for the LWR Loss-of-Coolant Accident, NUREG/CR-1298 (ORNL/NUREG/TM-321), July 1980.
6. M. F. Osborne, R. A. Lorenz, J. R. Travis, and C. S. Webster, Data Summary Report for Fission Product Release Test HI-1, NUREG/CR-2928 (ORNL/TM-8500), December 1982.

7. M. F. Osborne, R. A. Lorenz, J. R. Travis, C. S. Webster, and K. S. Norwood, Data Summary Report for Fission Product Release Test HI-2, NUREG/CR-3171 (ORNL/TM-8667), February 1984.
8. M. F. Osborne, R. A. Lorenz, K. S. Norwood, J. R. Travis, and C. S. Webster, Data Summary Report for Fission Product Release Test HI-3, NUREG/CR-3335 (ORNL/TM-8793), April 1984.
9. P. E. MacDonald to A. P. Malinauskas, Transmittal of CPL Assembly B05 Axial Flux Measurements, MacD-76-75, Sept. 11, 1975.
10. N. H. Larsen, Core Design and Operating Data for Cycles 1 and 2 of Peach Bottom-2, EPRI NP-563, June 1978.
11. R. L. Lines, ORNL, personal communication, June 28, 1978.
12. D. O. Campbell, ORNL, personal communication, Apr. 9, 1979.
13. V. W. Storhok, EG&G Idaho, personal communication, Mar. 12, 1979.
14. R. A. Lorenz and G. W. Parker, "Calculation of Amount of Radioactivity in Fuel Rod Void Spaces," in Nuclear Safety Program Annual Progress Report for Period Ending December 31, 1967, ORNL-4228, April 1968.
15. H. Albrecht, M. F. Osborne, and H. Wild, "Experimental Determination of Fission and Activation Product Release During Core Meltdown," Proceedings of Thermal Reactor Safety Meeting, Sun Valley, Idaho, Aug. 1-4, 1977.
16. P. Hofmann and D. Kerwin-Peck, "Chemical Interactions of Solid and Liquid Zircaloy-4 with UO_2 Under Transient Nonoxidizing Conditions," Proceedings of the International Meeting on Light Water Reactor Severe Accident Evaluation, Cambridge, Mass., Aug. 28-Sept. 1, 1983.
17. N. A. Lange, ed., Handbook of Chemistry, 9th ed., McGraw-Hill, New York, 1956, p. 1426.
18. I. Barin and O. Knacke, p. 254 in Thermochemical Properties of Inorganic Substances, Springer-Verlag, Berlin, New York, 1973.
19. J. L. Collins, calculation using JANAF data, January 1983.
20. Calculation using data of R. A. Sallach and R. Elrick, Sandia National Laboratory, personal communication to K. S. Norwood, 1983.
21. R. P. Wichner and R. D. Spence, Quantity and Nature of LWR Aerosols Produced in the Pressure Vessel During Core Heatup Accidents - A Chemical Equilibrium Estimate, NUREG/CR-3181 (ORNL/TM-8683), March 1984.

1

2

3

4

5

6

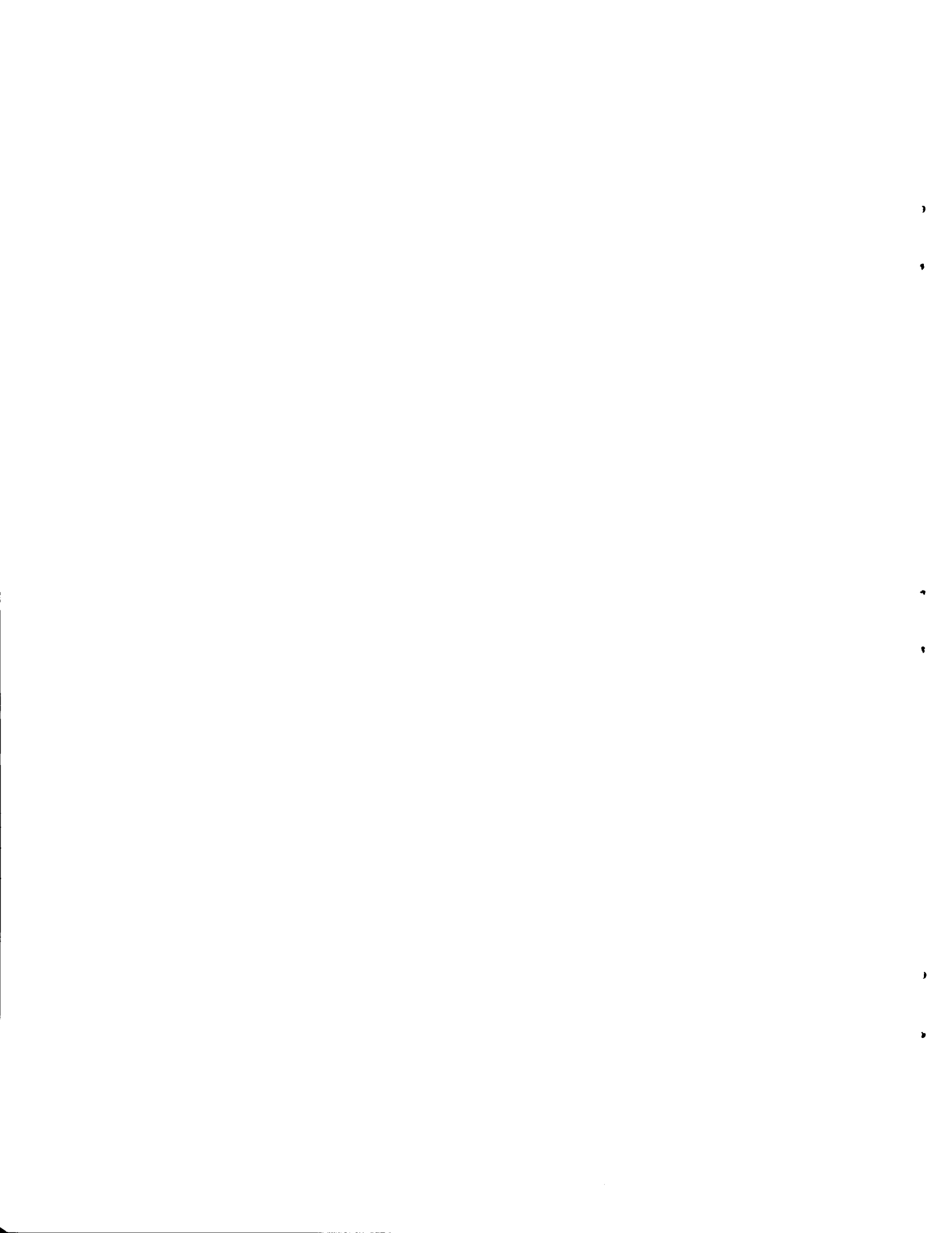
NUREG/CR-3600
 ORNL/TM-9011
 Dist. Category R3

INTERNAL DISTRIBUTION

- | | | | |
|--------|-------------------|-----|---|
| 1. | R. E. Adams | 28. | R. D. Spence |
| 2. | C. W. Alexander | 29. | M. G. Stewart |
| 3. | E. C. Beahm | 30. | O. K. Tallent |
| 4. | J. T. Bell | 31. | L. M. Toth |
| 5. | D. O. Campbell | 32. | R. L. Towns |
| 6-10. | J. L. Collins | 33. | J. R. Travis |
| 11. | G. E. Creek | 34. | C. S. Webster |
| 12. | J. R. Hightower | 35. | S. K. Whatley |
| 13. | T. S. Kress | 36. | R. P. Wichner |
| 14. | C. E. Lamb | 37. | R. G. Wymer |
| 15. | T. B. Lindemer | 38. | Central Research Library |
| 16-19. | R. A. Lorenz | 39. | ORNL-Y-12 Technical Library
Document Reference Section |
| 20. | A. P. Malinauskas | 40. | Laboratory Records |
| 21. | K. S. Norwood | 41. | Laboratory Records, ORNL RC |
| 22-26. | M. F. Osborne | 42. | ORNL Patent Section |
| 27. | J. H. Shaffer | | |

EXTERNAL DISTRIBUTION

43. Office of Assistant Manager for Energy Research and Development, ORO-DOE, P.O. Box E, Oak Ridge, TN 37831
- 44-45. Director, Division of Reactor Safety Research, U.S. Nuclear Regulatory Commission, Washington, DC 20555
- 46-47. Technical Information Center, DOE, Oak Ridge, TN 37831
48. Division of Technical Information and Document Control, U.S. Nuclear Regulatory Commission, Washington, DC 20555
49. L. K. Chan, U.S. Nuclear Regulatory Commission, Fuel Systems Research Branch, Division of Accident Evaluation, U.S. Nuclear Regulatory Commission, Washington, DC 20555
50. M. Jankowski, Fuel Research Systems Branch, Division of Accident Evaluation, U.S. Nuclear Regulatory Commission, Washington, DC 20555
51. R. V. Strain, Argonne National Laboratory, 9700 South Cass Avenue, Argonne, IL 60439
- 52-326. Given distribution as shown in Category R3 (NTIS - 10)



NRC FORM 335 (11-81)		U.S. NUCLEAR REGULATORY COMMISSION BIBLIOGRAPHIC DATA SHEET		1. REPORT NUMBER (Assigned by DDC) NUREG/CR-3600 ORNL/TM-9001	
4. TITLE AND SUBTITLE (Add Volume No., if appropriate) Data Summary Report for Fission Product Release Test HI-4				2. (Leave blank)	
7. AUTHOR(S) M. F. Osborne, J. L. Collins, R. A. Lorenz, K. S. Norwood, J. R. Travis, and C. S. Webster				3. RECIPIENT'S ACCESSION NO.	
9. PERFORMING ORGANIZATION NAME AND MAILING ADDRESS (Include Zip Code) Oak Ridge National Laboratory P.O. Box X Oak Ridge, TN 37831				5. DATE REPORT COMPLETED MONTH YEAR November 1983	
12. SPONSORING ORGANIZATION NAME AND MAILING ADDRESS (Include Zip Code) Division of Accident Evaluation Office of Nuclear Regulatory Research U.S. Nuclear Regulatory Commission Washington, D.C. 20555				6. (Leave blank)	
13. TYPE OF REPORT NUREG/CR and ORNL/TM				7. (Leave blank)	
15. SUPPLEMENTARY NOTES				8. (Leave blank)	
16. ABSTRACT (200 words or less) <p>The fourth in a series of high-temperature fission product release tests was conducted in which a 20.3-cm-long fuel specimen from the Peach Bottom-2 reactor was heated for 20 min at a maximum temperature of ~1850°C in a flowing steam-helium atmosphere. The test specimen was part of a fuel rod which was irradiated to ~10.10 MWd/kg.</p> <p>Posttest metallographic examination of the fuel specimen revealed evidence of cladding melting at each of the transverse cuts that were made. Gas analysis during the test indicated that ~54% of the cladding was oxidized. Total oxidation did not occur because of the low steam flow which was used.</p> <p>Gamma spectrometry (GS) and neutron activation (NA) analyses of test components revealed the following releases: (1) GS - 21.1% ⁸⁵Kr, 31.7% ¹³⁷Cs; and (2) NA - 24.7% ¹²⁹I (percentages of the total calculated segment inventories). A value of 35.8% cesium release was determined by counting the fuel rod segment before and after the test. If the pellet-clad gap fission gas inventory had also been available for release in the test, the ⁸⁵Kr release would have been 31.3%.</p> <p>Significant releases of radiogenic Rb, Cd, Ag, and Br, as well as trace amounts of Te, La, Ba, Sr, and Eu, were detected by spark-source mass spectrometric analysis.</p>				10. PROJECT/TASK/WORK UNIT NO.	
17. KEY WORDS AND DOCUMENT ANALYSIS Fission product chemistry Fission product release Severe LWR accident Fuel-cladding interaction Fuel damage				11. FIN NO. B0127	
17b. IDENTIFIERS/OPEN-ENDED TERMS				14. (Leave blank)	
18. AVAILABILITY STATEMENT				17a. DESCRIPTORS	
19. SECURITY CLASS (This report) Unclassified				21. NO. OF PAGES	
20. SECURITY CLASS (This page) Unclassified				22. PRICE S	